

See discussions, stats, and author profiles for this publication at: <https://www.researchgate.net/publication/230880267>

Regulation of late endosomal/lysosomal maturation and trafficking by cortactin affects Golgi morphology

ARTICLE *in* CYTOSKELETON · SEPTEMBER 2012

Impact Factor: 3.12 · DOI: 10.1002/cm.21051 · Source: PubMed

CITATIONS

11

READS

50

6 AUTHORS, INCLUDING:



[Kellye Kirkbride](#)

Vanderbilt University

23 PUBLICATIONS 768 CITATIONS

[SEE PROFILE](#)



[Nan Hyung Hong](#)

Vanderbilt University

7 PUBLICATIONS 382 CITATIONS

[SEE PROFILE](#)



[W. Gray \(Jay\) Jerome](#)

Vanderbilt University

119 PUBLICATIONS 3,047 CITATIONS

[SEE PROFILE](#)



[Alissa M Weaver](#)

Vanderbilt University

74 PUBLICATIONS 3,916 CITATIONS

[SEE PROFILE](#)



NIH Public Access

Author Manuscript

Cytoskeleton (Hoboken). Author manuscript; available in PMC 2013 September 01.

Published in final edited form as:

Cytoskeleton (Hoboken). 2012 September ; 69(9): 625–643. doi:10.1002/cm.21051.

Regulation of late endosomal/lysosomal maturation and trafficking by cortactin affects Golgi morphology

Kellye C. Kirkbride^{1,*}, Nan Hyung Hong^{1,*}, Christi L. French¹, Emily S. Clark^{1,^}, W. Gray Jerome², and Alissa M. Weaver^{1,2}

¹Department of Cancer Biology, Vanderbilt University Medical Center, Nashville, TN 37232, USA

²Department of Pathology, Microbiology and Immunology, Vanderbilt University Medical Center, Nashville, TN 37232, USA

Abstract

Cortactin is a branched actin regulator and tumor-overexpressed protein that promotes vesicular trafficking at a variety of cellular sites, including endosomes and the *trans*-Golgi network. To better understand its role in secretory trafficking, we investigated its function in Golgi homeostasis. Here, we report that knockdown (KD) of cortactin leads to a dramatic change in Golgi morphology by light microscopy, dependent on binding the Arp2/3 actin-nucleating complex. Surprisingly, there was little effect of cortactin-KD on anterograde trafficking of the constitutive cargo VSV-G, Golgi assembly from ER membranes upon Brefeldin A washout, or Golgi ultrastructure. Instead, electron microscopy (EM) studies revealed that cortactin-KD cells contained a large number of immature-appearing late endosomal/lysosomal (LE/Lys) hybrid organelles, similar to those found in lysosomal storage diseases. Consistent with a defect in LE/Lys trafficking, cortactin-KD cells also exhibited accumulation of free cholesterol and retention of the retrograde Golgi cargo M6PR in LE. Inhibition of LE maturation by treatment of control cells with Rab7 siRNA or chloroquine led to a compact Golgi morphology similar to that observed in cortactin-KD cells. Furthermore, the Golgi morphology defects of cortactin-KD cells could be rescued by removal of cholesterol-containing lipids from the media, suggesting that buildup of cholesterol-rich membranes in immature LE/Lys induced disturbances in retrograde trafficking. Taken together, these data reveal that LE/Lys maturation and trafficking is highly sensitive to cortactin-regulated branched actin assembly and suggests that cytoskeletal-induced Golgi morphology changes can be a consequence of altered trafficking at late endosomes.

Introduction

Actin assembly is increasingly recognized to play an integral role in membrane trafficking events, including vesicle formation, fission, transport, and fusion (Lanzetti 2007). The branched actin regulator and tumor-overexpressed protein, cortactin, is thought to be a key coordinator of membrane trafficking since it decorates branched actin networks throughout the cell and binds to a variety of membrane trafficking, signaling, and cytoskeletal proteins (Clark and Weaver 2008; Kirkbride et al. 2011; Lanzetti 2007). Indeed, a number of studies have shown that cortactin can regulate endocytic trafficking, including initial endocytosis from the plasma membrane (Cao et al. 2010; Cao et al. 2003; Engqvist-Goldstein et al.

Correspondence to Alissa Weaver: alissa.weaver@vanderbilt.edu.

*equal contribution

[^]Current address: University of Miami Medical School, Miami, FL, 33101

Online Supplemental Material – Supplemental Figure legends are embedded with the figures.

The authors have no conflict of interest to declare.

2004; Grassart et al. 2010; Merrifield et al. 2005; Sauvonnet et al. 2005; Zhu et al. 2007; Zhu et al. 2005) and recycling (Puthenveedu et al. 2010; Sung et al. 2011). Cortactin has also been shown to regulate secretion of several proteins that promote aggressive tumor phenotypes (Clark et al. 2009; Clark et al. 2007; Sung et al. 2011) and might utilize either Golgi (Cao et al. 2005; Salvarezza et al. 2009) or endocytic (Steffen et al. 2008; Sung et al. 2011) trafficking pathways. Two studies have shown that expression of a dominant-negative cortactin molecule that lacks the SH3 domain blocks exit of model cargo-containing vesicles from the *trans*-Golgi network (TGN) (Cao et al. 2005; Salvarezza et al. 2009), suggesting an important role for cortactin in actin assembly and trafficking at the Golgi. However, the overall role of cortactin in Golgi structure and function is poorly understood.

Perturbation of either actin assembly or actin binding to Golgi membranes leads to either compaction or fragmentation of the Golgi (Campellone et al. 2008; Dippold et al. 2009; Egea et al. 2006; Hayes and Pfeffer 2008; Lanzetti 2007; Lazaro-Dieguex et al. 2006; Valderrama et al. 1998); however, the underlying mechanisms are unclear. Although treatment with actin-targeting drugs typically leads to compaction of the Golgi by light microscopy, there is variation in the effects on cisternal ultrastructure including cisternal fragmentation or bloating depending on the drug (Lazaro-Dieguex et al. 2006; Valderrama et al. 1998). A variety of mechanisms have been proposed for these effects on the Golgi, including an essential role for actin in maintaining cisternal structure, intraluminal pH, and vesicular trafficking (Egea et al. 2006; Lazaro-Dieguex et al. 2006; Matas et al. 2004; Valderrama et al. 1998; Valderrama et al. 2001; Valderrama et al. 2000). Vesicular trafficking in particular seems a likely mechanism by which actin regulators control Golgi homeostasis, since a growing number of actin-associated molecules and actin regulators have been shown to affect both trafficking to or from the Golgi concomitant with Golgi morphology changes (Campellone et al. 2008; Hehnly et al. 2010; Warner et al. 2003).

The endocytic system communicates with the Golgi apparatus at multiple points (Pfeffer 2009). In addition to receiving essential cargo from the Golgi, a number of lipid and protein cargoes are returned to the Golgi from early and late endosomes. Indeed, proper homeostasis of the Golgi depends on intact function of endocytic trafficking. For example, in certain lysosomal storage diseases (LSD) such as Niemann-Pick disease type C (NPC), accumulation of cholesterol and other cargo in immature late endosomal/lysosomal (LE/Lys) hybrid organelles can lead to defective retrograde trafficking of mannose-6-phosphate receptor (M6PR) and other cargo to the Golgi apparatus (Choudhury et al. 2002; Ganley and Pfeffer 2006). A potential mechanism for the disturbance of LE trafficking by LSD is aberrant accumulation of assembled SNARE complexes that accompanies defective breakdown of cholesterol-rich lipid rafts (Fraldi et al. 2010).

In the present study, we investigated the role of cortactin in regulating Golgi morphology, size and trafficking. We found that knockdown (KD) of cortactin in several cell types leads to a substantial alteration in Golgi organization by light and electron microscopy; however stereology quantification indicated little alteration in Golgi apparatus size. In addition, trafficking of the model protein ts045-VSV-G (VSV-G) from the endoplasmic reticulum (ER) through the Golgi to the plasma membrane was unaffected, as was Brefeldin A (BFA)-induced assembly or disassembly of the Golgi in cortactin-KD cells. By contrast, EM studies revealed that cortactin-KD cells contained many enlarged LE/Lys hybrid organelles, suggesting a defect in LE/Lys maturation and trafficking. Likewise, cortactin-KD cells accumulated the retrograde LE-to-Golgi cargo M6PR as well as free cholesterol in LE. Inhibition of LE/Lys maturation by siRNA-depletion of the GTPase Rab7 or treatment with the lysosomotropic agent chloroquine induced a Golgi morphology phenotype that was identical to that of cortactin-KD cells. Furthermore, Golgi morphology defects of cortactin-KD cells were partially rescued by removing the LE/Lys cargo cholesterol from the culture

media. Reexpression of cortactin mutants in cortactin-KD cells revealed that cortactin binding to the actin-nucleating Arp2/3 complex is essential for rescue of Golgi morphology defects. These data are consistent with a model in which cortactin indirectly regulates Golgi homeostasis by controlling LE/Lys maturation and trafficking.

Results

Cortactin regulates Golgi morphology

To examine how cortactin regulates the Golgi, we began by immunostaining SCC61 head and neck squamous cell carcinoma (HNSCC) cells stably expressing either human cortactin-specific shRNA (cortactin-KD1 or – KD2), a scrambled oligo shRNA (scrambled) or a cortactin-specific shRNA along with an shRNA-insensitive mouse cortactin gene (KD1/rescue) (Fig. 1) (Bryce et al. 2005; Clark et al. 2007). By light microscopy, the Golgi in scrambled control SCC61 cells was dispersed around the nucleus, consistent with the reported Golgi morphology in aggressive cancer cells (Ayala et al. 1999). By contrast, loss of cortactin expression resulted in a dramatic change in Golgi morphology to a more compact perinuclear cluster, which was rescued by reexpression of shRNA-insensitive cortactin (Fig. 1B). Quantification of the ratio of total Golgi area to total cell area (Burman et al. 2010) showed that the Golgi occupies significantly less area within cortactin-KD SCC61 cells compared to scrambled oligo control cells and KD1/rescue cells (Fig. 1B).

Analysis of *cis*- (GM130, GRASP65), *medial*- (Mannosidase II) and *trans*-Golgi (p230^{trans}, GCC185) markers revealed that the morphology of the entire Golgi apparatus is altered in cortactin-KD cells (see Fig. S1A). The ER-Golgi intermediate compartment (ERGIC; ERGIC-53 as a marker) was also more compact in KD cells. There were no obvious changes in ER morphology, as assessed by immunostaining of calreticulin (Fig. S1A). We confirmed that our TGN antibodies mark the appropriate secretory compartment by low level transient expression of the TGN marker, TGN38–HRP (Connolly et al. 1994; Egorov et al. 2009), in both control and cortactin-KD cells. The localization of TGN38-HRP resembled that of p230^{trans} and GCC185, and further confirmed the compact TGN morphology in cortactin-KD cells (Fig. S1B).

Stable expression of cortactin shRNA in both HeLa cervical cancer and MCF10A breast epithelial cells also led to a more compact Golgi morphology, indicating that the effect of cortactin-KD was not unique to SCC61 or HNSCC cells (Fig. 1B). We also tested the effect of transient expression of cortactin-specific siRNA on Golgi morphology (Fig. 1C). In SCC61 cells transfected with cortactin-specific siRNA for 72 h, the phenotype was identical to that of stable cortactin shRNA expression with a decrease in Golgi area. By contrast, in HeLa cells, which under normal conditions have a more compact Golgi than SCC61 cells, transient expression of cortactin siRNA led to an increased ratio of Golgi area to cell area. It is unclear why HeLa cells have an opposite response to transient versus stable KD of cortactin. However, we can conclude from these data that loss of cortactin affects Golgi homeostasis over both a short-term (Fig. 1C) and long-term (Fig. 1B) timescale.

Cortactin is not essential for Golgi assembly from ER membranes or VSV-G transport to the plasma membrane

One possible explanation for the altered Golgi morphology of cortactin-KD cells is that cortactin affects membrane flow and/or Golgi assembly from ER membranes (Guo and Linstedt 2006; Lowe 2002), leading to a net decrease in the size of the Golgi compartment over time. To test the possibility of altered membrane flow from the ER to the Golgi, we performed a BFA washout assay in which control and stable cortactin-KD cells were incubated with 5 µg/ml BFA to disassemble the Golgi and allow fusion with the ER

(Klausner et al. 1992). After 30 min, the BFA was washed out and cells were fixed and immunostained for the Golgi marker GM130 (Fig. 2) at various timepoints. In both control and cortactin-KD cells, the Golgi was effectively dispersed by treatment with BFA (compare “control” to “+BFA” images, Fig 2). Likewise, the Golgi in both scrambled and cortactin-KD HeLa and SCC61 cells reassembled after BFA washout (compare “120 min” to “+BFA” images, Fig 2). Note that the Golgi morphology of cortactin-KD cells is more compact after BFA washout, indicating a return to steady state morphology by 120 min (compare “120 min” to “control” images). Overall, these data indicate that cortactin is not essential for BFA-induced Golgi disassembly or for reassembly from ER membranes.

To further test whether trafficking from the ER to the Golgi and forward to the plasma membrane (PM) was impaired in cortactin-KD cells, we analyzed synchronized trafficking of the model constitutive cargo protein ts045-VSV-G-GFP (VSV-G) in stable KD and control SCC61 and HeLa cells. As previously described (Hirschberg et al. 1998; Presley et al. 1997), cells were transiently transfected with temperature-sensitive VSV-G plasmid and incubated at the restrictive temperature (40°C) to induce retention of expressed VSV-G in the ER (Fig. 3A, **0 min**, see also Fig S2A). A temperature shift to the permissive temperature (32°C) allows proper folding of the extracellular domain and subsequent transport of VSV-G to the Golgi and then to the PM (Hirschberg et al. 1998; Presley et al. 1997). At various time points after the temperature shift, live unpermeabilized cells were incubated for 10 min with a monoclonal antibody that recognizes the extracellular domain of VSV-G (I14, (Feinstein and Linstedt 2008)) and then fixed and processed for immunofluorescence. This method allows specifically detection of only the PM-localized pool of VSV-G (Feinstein and Linstedt 2008) by I14 staining as well as intracellular localization using the GFP tag. At the 0 min time point, VSV-G on the PM was minimal as determined by I14 staining and retained in the ER in both SCC61 and HeLa cells (Fig 3A; Fig S2A, respectively). However, over time in both cell types, there was movement of GFP-VSV-G from the ER to the Golgi (compare localization patterns of VSV-G-GFP at 0 min and 60 min in Fig. 3A) and an increase in PM VSV-G staining (Fig. 3A, Fig. S2A, I14 staining). Surprisingly, there was no difference between control and cortactin-KD cells in the rate of appearance of VSV-G at the PM as quantitated from I14 staining (Fig. 3B) (Cao et al. 2005). These data indicate that cortactin is not an essential regulator of ER-to-Golgi or Golgi-to-PM trafficking, at least for the major anterograde transport route utilized by VSV-G (Ponnambalam and Baldwin 2003).

EM analysis reveals minimal changes in Golgi ultrastructure or volume, and an abundance of immature LE/Lys hybrid organelles

The changes in Golgi morphology identified in cortactin-KD cells by light microscopy could represent a variety of organizational, size, or structural changes in the Golgi apparatus. In order to determine whether cortactin affects Golgi structure or size, we performed transmission EM on 50 nm sections obtained from control and cortactin-KD SCC61 and HeLa cells (Fig. 4 **and** Fig. S2B–E, respectively). Surprisingly, loss of cortactin did not dramatically alter the structure of the Golgi stacks, although there was a subtle increase in *cis*- and *trans*-Golgi-associated coated and non-coated vesicles in KD cells (Fig 4A,B, zoom shows TGN-associated traffic). To determine whether Golgi size was altered in cortactin-KD cells, we performed point counting morphometry analysis on random thin sections (Jerome et al. 1998; Weibel et al. 1969) and quantitated the percent volume of the cytoplasm occupied by Golgi elements. For both SCC61 and HeLa cells, there was a small decrease in the Golgi volume; however this difference was only statistically significant in SCC61 cells, possibly due to variability in Golgi volume between HeLa samples. A more obvious change in both SCC61 and HeLa cortactin-KD cells was a large and statistically significant expansion in the number and size of LE/Lys hybrid organelles (asterisks in images in Fig. 4,

Fig. S2B–E) containing excess membrane and undigested cellular elements. This morphological phenotype is reminiscent of lysosomal storage diseases such as Niemann-Pick C, in which lamellar bodies, autophagolysosomes, and other immature LE/Lys hybrid organelles fill the cytoplasm. Consistent with our morphological identification of LE/Lys, by light microscopy cortactin-KD cells contain enlarged Rab7/LAMP1-double positive LE/Lys compartments (Fig S3) (Sung et al. 2011). Interestingly, when challenged by a dextran pulse, the large LE/Lys compartments in cortactin-KD cells are studded with small vesicles containing dextran, but do not contain dextran themselves (Fig S3), suggesting a storage-disease-like fusion defect (Heard et al. 2010; Vitry et al. 2010). Overall, these data suggest that cortactin-KD cells exhibit a profound perturbation in LE/Lys maturation and/or trafficking and more minor changes in Golgi size and organization.

Cortactin colocalizes with a subset of late endosomal markers

Since loss of cortactin did not have a major effect on anterograde trafficking or Golgi ultrastructure, we hypothesized that cortactin may not act directly on the Golgi to regulate its morphology (the major Golgi phenotype that we observed). Instead, the compact Golgi morphology that we observed in cortactin-KD cells might be the consequence of altered retrograde membrane flow back to the Golgi, potentially from LE/Lys. To determine which compartments cortactin is associated with and thus might be regulating, parental SCC61 cells were fixed and immunostained for cortactin and a variety of markers, including Golgi, ER, LE and Lysosomes. Single confocal images were then analyzed for colocalization. Consistent with previous reports, cortactin localizes to the cell periphery as well as to perinuclear puncta (Weed and Parsons 2001) (Fig. S4). There was no apparent overlap between cortactin staining and ER (calreticulin), ERGIC (ERGIC53), or *cis*/medial-Golgi (GM130, Mannosidase II) compartments (Fig. S4). For the TGN, there was a small amount of cortactin colocalization with GCC185 but not with p230^{trans} (Figs S5A and S4, respectively). In addition, we found that cortactin colocalizes with and is adjacent to a subset of Rab7-positive and LAMP1-positive (Fig. S5B and S5C) vesicles. Since retrograde trafficking to the Golgi from LE/Lys compartments involves docking with GCC185 at the TGN (Derby et al. 2007; Reddy et al. 2006), these colocalization data suggest that cortactin might be involved in LE/Lys-to-Golgi trafficking.

Cortactin regulates localization of mannose-6-phosphate receptor (M6PR)

To directly test whether cortactin promotes LE-to-Golgi trafficking, we analyzed in cortactin-manipulated cells the localization of a canonical marker of that pathway: mannose-6-phosphate receptor (M6PR). M6PR molecules are required for transport of lysosomal hydrolases from the TGN and are returned to the TGN from LE (Pfeffer 2009). Consistent with the hypothesis that cortactin is critical for trafficking from LE to the TGN, there was a significant increase in M6PR localization to LE (marked by Rab7) in cortactin-KD cells compared to control cells (Fig. 5). Likewise, M6PR localization to the TGN (marked by Giantin) was significantly reduced in cortactin-KD cells compared to control cells (Fig. 5). These data suggest that cortactin plays a role in trafficking of M6PR back to the Golgi from LE/Lys.

Inhibition of LE/Lys maturation leads to a similar compact Golgi morphology as that of cortactin-KD cells

To formally test whether inhibition of LE/Lys maturation and trafficking could affect Golgi morphology, we treated SCC61 cells with siRNA targeting the late endosomal GTPase Rab7. Rab7 is essential for maturation and trafficking from LE (Vanlandingham and Ceresa 2009; Zhang et al. 2009) and a dominant negative mutant of Rab7 causes the accumulation of M6PR in early endosomes (Press et al. 1998). Similar to the effects of cortactin-KD, Rab7 siRNA transfection led to a compact Golgi morphology in SCC61 cells (Fig. 6A,B).

We also tested whether inhibition of LE/Lys maturation with the lysosomotropic agent chloroquine (Blok et al. 1981a; Blok et al. 1981b; Brown et al. 1984; Kokkonen et al. 2004) could affect Golgi morphology. Indeed, 12 h treatment of SCC61 cells with 60 μ M chloroquine led to an overall decrease in the Golgi area to cell area ratio measured by GM130 staining (Fig. 6C) that phenocopied the Golgi morphologies of cortactin-KD and Rab7 siRNA-treated cells (Figs. 1 and 6A).

To further test whether LE maturation and trafficking regulates Golgi morphology, we determined the effect of Rab7 transient siRNA treatment in HeLa cells. Whereas stable KD of cortactin in SCC61, HeLa, and MCF10A cells (Fig 1B) and transient KD of cortactin in SCC61 cells (Fig 1C) all cause a compact Golgi morphology by light microscopy, transient cortactin-KD in HeLa cells instead causes an increase in the Golgi area to cell area ratio (Fig. 1C). Thus, we reasoned that a robust test of whether LE maturation and trafficking regulates Golgi morphology would be to determine whether transient KD of Rab7 in HeLa cells mimics the paradoxical increase in Golgi area/cell area seen with transient cortactin-KD. Indeed, transient Rab7-KD in HeLa cells (Fig 6A) did phenocopy transient cortactin-KD, causing an increase in the Golgi area/cell area ratio and greater distribution of the Golgi around the nucleus by light microscopy (Fig. 6D).

Finally, we also tested the effect of Rab9 siRNA on Golgi morphology. Whereas Rab7 is critical for LE maturation, which is essential for subsequent LE trafficking, Rab9 is critical for retrograde trafficking of M6PR and other cargo from Rab7-positive LE to the Golgi (Pfeffer 2009; Vanlandingham and Ceresa 2009). Therefore, we also tested the effect of Rab9 siRNA on Golgi morphology. Interestingly, transient KD of Rab9 in SCC61 cells had no effect on Golgi morphology (Fig 7). In HeLa cells, Rab9 siRNA treatment did lead to an increase in Golgi area/cell area, but the organization of the Golgi was distinct from that of HeLa cells treated with siRNA to Rab7 or cortactin (Fig 7B compared to Fig 1C and 6B). These data suggest that cortactin functions upstream of Rab9-mediated trafficking, at the level of LE maturation similarly or alongside Rab7. Consistent with that model, our EM analysis revealed the presence of many enlarged immature LE/Lys in cortactin-KD cells (Fig 4, fig S2B–E).

Regulation of cholesterol homeostasis by cortactin is linked to Golgi morphology changes

A key function of LE is metabolism and trafficking of cholesterol-rich membranes. In lysosomal storage diseases, a buildup of free cholesterol in LE/Lys hybrid organelles has been shown to affect endosomal dynamics, homeostasis of glycosphingolipids and retrograde trafficking to the Golgi (Choudhury et al. 2002; Ganley and Pfeffer 2006; Kobayashi et al. 1999). To determine whether cortactin affects cholesterol homeostasis, we stained control and cortactin-KD cells for free cholesterol using filipin. In both cell types, filipin stained intracellular vesicles as well as the plasma membrane (Fig 8A). Interestingly, compared with controls, SCC61 cortactin-KD cells contained enlarged and bright intracellular filipin-positive vesicles (arrows, Fig 8A), suggesting a defect in cholesterol metabolism or trafficking. In HeLa cells, the pattern of filipin staining was altered by cortactin-KD, with increased clustering of the filipin-positive vesicular pattern.

To determine whether the buildup of cholesterol in cortactin-KD cells was connected to the Golgi morphology changes, we performed a rescue experiment in which exogenous cholesterol was removed from the cellular environment. Control and cortactin-KD cells were cultured in media containing lipid-depleted or full serum for 96 h and Golgi area/cell area was analyzed. In control SCC61 and HeLa cells, there was no significant effect on Golgi morphology of culturing in lipid-depleted serum (Fig 8B,C). By contrast, culturing cortactin-KD cells in lipid-depleted serum led to either a complete (SCC61 KD2, HeLa KD1) or partial (SCC61 KD1) rescue in Golgi morphology, as quantitated by Golgi area/cell

area. These data suggest that defective cholesterol homeostasis in cortactin-KD cells is responsible for Golgi morphology changes.

Cortactin binding to the Arp2/3 complex is essential to regulate Golgi morphology

Cortactin is a well-known regulator of branched actin assembly and also binds a number of membrane trafficking and signaling proteins (Kirkbride et al. 2011). Several proteins known to interact with cortactin have also been shown to regulate Golgi morphology, including src family kinases, actin and Dynamin-2 (Bard et al. 2003; Valderrama et al. 1998; Weller et al. 2010). Both loss of expression of src family kinases (Bard et al. 2003) and treatment of cells with actin depolymerizing drugs (Valderrama et al. 1998) result in a compact Golgi morphology similar to that seen in cortactin-KD cells. To identify which binding interactions are required for regulation of Golgi morphology by cortactin, we re-expressed shRNA-resistant mouse cortactin constructs with point mutations or small deletions at key binding sites (Bryce et al. 2005; Kinley et al. 2003; Weed et al. 2000) in cortactin-KD SCC61 cells (Fig. 9A,B). Re-expression of either wild-type cortactin or the src phosphorylation (3Y) mutant rescued the knockdown phenotype, with a redistribution of the Golgi around the periphery of the nucleus and an increase in Golgi area/cell area (Fig. 9C,D). In contrast, the Arp2/3-binding (W22A) mutant was unable to rescue the phenotype and retained the compact perinuclear cluster phenotype of cortactin-KD cells (Fig. 9C,D). The SH3 domain (W525K) and actin-binding (Δ 4RP) cortactin mutants had intermediate phenotypes that were difficult to classify as either rescued or not. We suspect that there may be a dominant negative effect of these two mutants that leads to a large amount of cell-to-cell variability in terms of both cell and Golgi areas (Fig. 9C). Taken together, these data indicate that cortactin regulates Golgi morphology via interaction with the branched actin nucleator Arp2/3 complex. Although src kinase may indeed be involved generally in regulation of Golgi morphology (Bard et al. 2003; Weller et al. 2010), phosphorylation of cortactin at the canonical src sites does not appear to be essential.

Discussion

Cortactin is an actin regulatory protein that has recently been implicated in promoting secretion of proteases, ECM and growth factors (Clark et al. 2009; Clark et al. 2007; Sung et al. 2011). Since a likely mechanism was control of Golgi-mediated secretion (Cao et al. 2005; Salvarezza et al. 2009), we examined the consequence of cortactin loss on Golgi function and homeostasis. To our surprise, we found that cortactin-KD in two different cell types did not affect the anterograde constitutive transport pathway utilized by VSV-G through the Golgi en route to the PM. Cortactin-KD also had no apparent effect on Brefeldin A-induced Golgi disassembly or reassembly from ER membranes and little effect on the structure of Golgi stacks. Instead, we found that a consistent and major effect of cortactin loss on the Golgi was to alter its light microscopy morphology, most likely by an indirect mechanism involving defective cholesterol trafficking at LE/Lys compartments. Consistent with a block in LE/Lys maturation and/or trafficking, cortactin-KD cells contained enlarged LE/Lys and cholesterol-containing compartments and accumulation of the endosome-to-Golgi retrograde cargo M6PR in LE. Furthermore, removal of cholesterol from the culture media rescued the Golgi morphology defects of cortactin-KD cells. Altogether these data suggest a model in which cortactin regulates LE/Lys cholesterol trafficking, which subsequently impacts Golgi homeostasis.

The phenotype that we noted in cortactin-KD cells, with enlargement of an immature membrane-filled LE/Lys compartment, intracellular accumulation of free cholesterol, and alteration in Golgi homeostasis is reminiscent of that seen in cells with lysosomal storage diseases (Mukherjee and Maxfield 2004). For example, Niemann-Pick C disease occurs due to a specific defect in cholesterol transport out of LE/Lys that results in defective transport

of retrograde cargo to the Golgi, including glycosphingolipids and M6PR (Choudhury et al. 2002; Ganley and Pfeffer 2006; Kobayashi et al. 1999). Indeed we find that removal of cholesterol from the endocytic system by culturing cortactin-KD cells in lipoprotein-deficient serum led to a partial rescue of Golgi morphology defects. Interestingly, recent data shows that accumulation of cholesterol occurs in cells with diverse lysosomal storage diseases and leads to accumulation of aberrant assembled SNARE complexes on LE/Lys (Fraldi et al. 2010), which may explain how gross changes in retrograde trafficking (Choudhury et al. 2002; Ganley and Pfeffer 2006; Kobayashi et al. 1999; Mukherjee and Maxfield 2004) and Golgi morphology could occur. Since cortactin is an actin regulator that is known to regulate endosomal tubulation and trafficking (Ohashi et al. 2011; Puthenveedu et al. 2010), it seems likely that cholesterol accumulation in cortactin-KD cells occurs secondary to LE/Lys maturation and/or trafficking defects rather than by direct regulation of cholesterol transport. Consistent with that idea, inhibition of LE/Lys maturation with Rab7 siRNA or chloroquine treatment (Huotari and Helenius 2011; Vanlandingham and Ceresa 2009; Zhang et al. 2009) led to a similar Golgi morphology change as cortactin-KD. However, it will be important in the future to determine exactly how actin dynamics, regulated by cortactin, controls cholesterol homeostasis and trafficking at LE.

To understand the morphological changes we observed by light microscopy in cortactin-KD cells, we performed point counting morphometry analysis of EM images. Although there was a small change in Golgi volume measured by this method, it was insufficient to fully account for the large changes in Golgi area/cell area that was observed by light microscopy. One possible reason for the discrepancy between the two methods is that light microscopy is detecting primarily changes in Golgi distribution (spread out versus compact). Since EM has higher resolution, it is a more accurate method for determining volume than light microscopy (Quinn et al. 1983; Weibel 1979). Another possibility, which is not mutually exclusive, is that some of the Golgi marker staining is actually labeling the LE/Lys compartment because membrane flow is altered. Indeed, a compartment that includes both Golgi and LE/Lys components was first identified as the ‘GERL’ (Golgi–ER–lysosomal compartment) described by Alex Novikoff in 1964 (Novikoff et al. 1964) and may become expanded in certain situations, such as neuronal storage diseases (Vitry et al. 2010) and Ras-transformation (Narita et al. 2011). Additional future studies are required to distinguish between these two possibilities; however our data indicate that either way LE/Lys dysfunction is responsible for the light microscopy Golgi morphology changes.

Molecules that directly regulate the actin cytoskeleton have been previously shown to significantly affect Golgi morphology. In particular, studies by several different groups have shown that treatment with toxins that affect actin dynamics/stability or siRNA-mediated KD of actin-associated proteins leads to compaction of the Golgi in a similar manner to that described here in cortactin-KD and Rab7-KD cells (di Campli et al. 1999; Dippold et al. 2009; Egea et al. 2006; Lazaro-Dieguet et al. 2006; Valderrama et al. 1998). While it is certainly likely that some of the reported phenotypes are due to direct regulation of Golgi actin, we speculate that in some cases the common “compacted” morphology may be a secondary consequence of disturbed lipid trafficking secondary to LE/Lys maturation defects. The cortactin-KD phenotype depended on interactions with Arp2/3 complex, suggesting that regulation of branched actin networks is critical. Interestingly, both the Arp2/3 complex and actin filaments have been shown to regulate late endosomal size, shape and maturation (Duleh and Welch 2010; Holtta-Vuori et al. 2005), all phenotypes that are consistent with the expansion of LE/Lys in cortactin-KD cells and the reported role of cortactin in autophagosome-lysosome fusion (Lee et al. 2010). Such alterations in late endosome maturation would necessarily affect trafficking to other sites, including the Golgi. Indeed, Rab7-KD is known to block late endosomal maturation and trafficking (Vanlandingham and Ceresa 2009) and in this study phenocopied the effect of cortactin-KD

on Golgi morphology. Based on our data, we speculate that LE/Lys maturation and trafficking may be particularly sensitive to actin dynamics.

An unexpected finding of this study was that cortactin did not affect trafficking of VSV-G to the PM or, in our system, colocalize with most Golgi markers. Interestingly, the one TGN marker for which we did observe cortactin colocalization is GCC185, a Golgin tether that binds M6PR-containing vesicles returning from late endosomes (Derby et al. 2007; Reddy et al. 2006). Our VSV-G transport data were unexpected since two previous studies found that expression of a dominant mutant of cortactin that lacks 50 amino acids of the SH3 domain leads to a block in the exit of VSV-G (Cao et al. 2005) or p75-GFP cargo (Salvarezza et al. 2009) from the TGN. Expression of the same mutant also led to bloated TGN cisternae, consistent with a Golgi exit block (Cao et al. 2005; Salvarezza et al. 2009). By contrast, despite a >95% knockdown of cortactin levels in stable HeLa and SCC61 cells, we observed no difference in the rate of VSV-G arrival at the PM and Golgi ultrastructure was relatively normal (Fig 4), albeit with some accumulation of vesicles at the cis- and trans-Golgi. Our data suggest that in the absence of cortactin, molecular trafficking components regulating anterograde bulk transport remain functional. The most probable explanation for the difference in our findings from those of previous studies is the use of dominant negative mutants versus knockdown of endogenous proteins. We speculate that the dominant-negative cortactin mutant decreases TGN exit by either sequestering critical factors (such as Arp2/3 complex or Src kinase) or masking Golgi-associated branched actin networks that function as recruitment platforms for Dynamin-2 or other critical proteins (Cao et al. 2005; Salvarezza et al. 2009). Additionally, it is certainly possible that cortactin regulates the transport of other cargo from the Golgi, similar to the cargo sorting role reported for cofilin (von Blume et al. 2009). Finally, it is possible that cortactin functions at the Golgi are redundant with another similar protein, such as mAbp1 that can link actin filaments to dynamins (Kessels et al. 2001; Onabajo et al. 2008) and is recruited to dynamic actin at the Golgi (Fucini et al. 2002; Xu and Stamnes 2006). Indeed, the fact that we found little colocalization of cortactin with any Golgi marker in our squamous carcinoma (SCC61, HeLa) and basal mammary epithelial (MCF10A) cells suggests that other actin-binding proteins may be utilized for recruitment of the fission machinery to the Golgi. Further studies will be required to distinguish between these possibilities.

Cortactin is a prominent Src kinase substrate and is frequently involved in Src-regulated cellular processes (Kirkbride et al. 2011; Wu et al. 1991). Similar to cortactin-KD cells, fibroblasts lacking the src family kinases Src, Yes, and Fyn exhibit a compact Golgi morphology (Bard et al. 2003). Likewise, expression of a constitutively active Src kinase was recently shown to lead to Golgi fragmentation (Weller et al. 2010). Therefore, we were surprised that a cortactin mutant that cannot be phosphorylated by Src kinase (Kinley et al. 2003) fully rescued the Golgi morphology defect of cortactin-KD cells. One possibility is that both proteins still act in concert but that Src phosphorylation of cortactin is not necessary for cortactin regulation of Golgi morphology (Martinez-Quiles et al. 2004). Consistent with that possibility, a large pool of Src kinase is associated with late endosomes (Sandilands and Frame 2008) and may regulate movement and distribution of lysosomes (Nakayama et al. 1994; Vincent et al. 2007). Alternatively, Src kinase may directly regulate intra-Golgi and Golgi-to-ER trafficking (Bard et al. 2003; Pulvirenti et al. 2008).

Cortactin is well-studied as a regulator of cancer aggressiveness and invasiveness (Kirkbride et al. 2011). One particular focus of the field has been the role of cortactin as a regulator of invadopodia, specialized actin-rich structures with associated extracellular matrix (ECM)-degrading activity (Weaver 2006). Our interest in the role of cortactin in exocytosis stemmed from our finding that cortactin is essential for secretion of the invadopodia-localized proteinases, MMP2, MMP9, and MT1-MMP (Clark et al. 2009; Clark and Weaver

2008; Clark et al. 2007). Thus, it was initially surprising that cortactin is not an essential regulator of Golgi exit, at least not for VSV-G. However, MT1-MMP trafficking to invadopodia was recently shown to depend on the LE/Lys SNARE VAMP7 (Steffen et al. 2008). In addition, both MT1-MMP and MMP9 have been localized to a LE/Lys compartment (Sbai et al. 2009; Steffen et al. 2008). Furthermore, we recently found that the extracellular matrix component fibronectin (FN) can be endocytosed and resecreted from a LE/Lys compartment to promote cell motility, dependent on cortactin (Sung et al. 2011). Therefore, it seems likely that regulation of LE/Lys trafficking is a major function of cortactin that is important not only for Golgi homeostasis but also for cellular motility and invasiveness.

Materials and Methods

Constructs, Antibodies, and Reagents

The construct encoding HRP-TGN38 was a gift from Dan Cutler (UCL) and the temperature-sensitive VSV-G (ts045-VSV-G-GFP) was a gift from Jennifer Lippincott-Schwartz (NIH). The conformation-specific mouse monoclonal anti-VSV-G antibody (I14) was provided by Anne K. Kenworthy (Vanderbilt University, Nashville, TN). Calreticulin (ab2907) and mannosidaseII (ab12277) antibodies were from abcam. Mouse anti-cortactin (mouse 4F11) was from Millipore. Rabbit anti-cortactin (H-191), GRASP65 (sc-30093), and ERGIC-53 (sc-32442) were from Santa Cruz. The GM130 and p230^{trans} (611280) antibodies were from BD Transduction Labs, Rab7 antibody (R8779) was from Sigma, and the goat anti-HRP (123-005-021) was from Jackson Immunoresearch Labs. GCC185 was a generous gift from Irina Kaverina (Vanderbilt). Cycloheximide (Calbiochem Co.) was stored as 1 mg/ml stock solution in methanol. Control (D-001210-02-05), cortactin (M-010508-00-005), Rab7a (M-010388-00-0005), and Rab9 (M-004177-01) siGENOME SMARTpool siRNA constructs were obtained from Thermo Scientific. Cortactin mutant cDNAs were obtained from Dr. J Thomas Parsons and subcloned into LZRS retroviral vector, as previously described (Bryce et al. 2005).

Cell Lines

SCC61 cells were maintained in DMEM supplemented with 20% fetal bovine serum (FBS), 0.4 µg/mL hydrocortisone, and 4 µg/mL puromycin (for stable cell lines) and 600 µg/mL G418 (for stable cortactin rescue cell lines). HeLa cells were maintained in RPMI 1640 supplemented with 10% bovine growth serum (BGS) and 4 µg/ml puromycin. MCF10A cells were maintained in DMEM/F12 supplemented with 5% horse serum, cholera toxin (0.1 µg/mL), insulin (1 mg/mL), hydrocortisone (0.5 µg/mL) and EGF (20 ng/mL). Stable cell lines were generated as previously described (Bryce et al. 2005; Clark et al. 2007). All cells were maintained at 37°C in 5% CO₂.

Transient Transfection and Drug Treatments

For all assays, including drug treatments, cells were plated on uncoated (HeLa) or fibronectin-coated (50 µg/mL; SCC61) glass coverslips for 18 h. For drug treatment assays, the cells were either treated with BFA or chloroquine, as indicated in the Results, before fixation and immunostaining. For TGN38-HRP, FLAG-tagged cortactin and GFP-Rab7 transfection, cells were transfected with 0.5 µg/well of cDNA using Lipofectamine2000 (Invitrogen) followed by fixation and immunostaining 24 h later with either an anti-FLAG or an anti-HRP antibody. For siRNA assays - control, cortactin (200 nM, 72 h), Rab9 (200 nM, 96 h) or Rab7a (100 nM, 48 h) siRNA were transfected into SCC61 and HeLa parental cells using Oligofectamine (Invitrogen). For Rab9 analyses, only cells with obvious loss of Rab9 expression determined by immunofluorescence were used in the quantification.

Widefield/Confocal Microscopy and Image Analysis

Cells were seeded (50,000) on coverslips. After 24 h, the cells were fixed in either 4% paraformaldehyde or methanol (Mannosidase II), permeabilized with TritonX100 or saponin (p230^{trans}), incubated with primary and secondary antibodies for 1 h each at room temperature. Hoechst was added on the last wash for 5 min and the coverslips were then mounted using Aqua Poly/Mount (Polysciences, Inc.). Secondary antibodies used were: goat anti-mouse Alexa Fluor 488 (GM130, cortactin (4F11), ERGIC-53, p230trans); goat anti-mouse Dylight 633 (for p230trans); goat anti-rat Alexa Fluor 546 (for LAMP2); goat anti-rabbit Alexa 488 (for M6PR, calreticulin (Golgi area)); goat anti-mouse Alexa Fluor 594 (LAMP1); goat anti-rabbit Alexa Fluor 594 (for FLAG, Mannosidase II, GRASP65, calreticulin (colocalization); cortactin (colocalization; H-191)); donkey anti-guinea pig 488 (GCC185); donkey anti-goat Alexa Fluro 488 (HRP). For filipin staining, cells were plated on coverslips for 24 hours, fixed in 3% PFA for 1 hour, quenched with glycine (1.5 mg/mL) and stained with filipin (0.05 mg/mL) for 2 hours at room temperature and imaged under UV light.

Images for quantification of Golgi area were acquired with an Eclipse TE2000-E wide-field fluorescent microscope (Nikon) equipped with a Plan Apo VC 60x, 1.4NA, oil immersion lens and a cooled charge-coupled device (CCD) camera (HAMAMATSU, C4742-80-12AG) by the use of *Metamorph* software. Golgi area was quantitated by thresholding the images based on GM130 and a goat anti-mouse Alexa Fluor 488 staining. Cell area was determined manually by tracing the cell perimeter in rhodamine-phalloidin stained images (not shown in most figures), and the ratio of Golgi to Cell area was calculated based on the thresholded area using *Metamorph* software. For colocalization experiments, images were acquired on a confocal laser scanning microscope (model LSM 510; Carl Zeiss, Inc.), using a Plan-APOCHROMAT 63x/1.4 oil DIC objective and either a Argon/2, HeNe1 and/or HeNe2 laser. Z-axis sectioning was at 0.2 μm intervals. Colocalization experiments were quantitated using *MetaMorph* software after thresholding images to remove background. Colocalization Image J plugin was used to show colocalized pixels between two images. Colocalized pixels were displayed as white on RGB overlay images.

Electron Microscopy (Stable shRNA KD cells; Conventional TEM)

Cells (1×10⁶) were plated on 10 cm dishes and 24 h later were fixed in 2.5% glutaraldehyde in 0.1 M Cacodylate buffer with 1% CaCl for 1 h at room temperature. The fixation buffer was then replaced with fresh buffer and incubated overnight at 4°C. The samples were scraped and transferred to conical tubes and washed extensively followed by osmifications for 1 h in 1% aqueous osmium tetroxide. The samples were then washed extensively followed by en bloc stained in ethanolic uranyl acetate for 10 min. The cells were dehydrated by passage through a graded series of increasing concentrations of ethanol. Dehydration was continued through increasing concentrations of ethanol. After the samples were embedded in epon resin and polymerized, cells were thin sectioned (50 nm) and imaged using a CM12 transmission EM (Philips) equipped with an AMT 542 camera.

Morphometry analysis of Golgi and LE/Lys area—Point counting stereology was used to quantitate relative volume of cytoplasm occupied by Golgi or LE/Lys elements (Jerome et al. 1998; Weibel et al. 1969). Thin sections from two independent blocks per cell line were randomly imaged for analysis. Additionally, one of the blocks was analyzed using two different sections. The magnification of images was optimized such that a point of the grid would fall on identifiable organelle structures. All micrographs used for stereology were 40,000×. A grid of intersecting lines (squares = 0.25 μm²) was superimposed using ImageJ Grid Plugin on each micrograph and the number of intersection points that fell on cytoplasm and organelles of interest were counted. From each section 30 micrographs/cell

line/section were collected in an unbiased manner and counted. The ratio: # points (organelle)/# points cytoplasm (minus the nucleus) was used to calculate a fractional cell cytoplasmic volume occupied by Golgi or LE/Lys. Student's t-test was used to determine the significance of the data.

VSV-G Trafficking Assay

SCC61 and HeLa cells were transiently transfected (0.75 mg/well in a 6-well dish containing glass coverslips) with a construct encoding ts045 VSV-G-GFP cDNA, and incubated for 16 h at 40°C. Cells were then treated with 100 µg/ml of cycloheximide for 30 min to stop protein synthesis and then shifted to 32°C for 0, 30, 45, 60, 120, or 180 min prior to fixation to allow transport of the nascent VSV-G through the secretory pathway. For determination of surface VSV-G, live cells were incubated with an antibody (I14) directed against the luminal domain of VSV-G for 10 min at 4°C, washed extensively, fixed, and stained with an Alexa 594 secondary antibody. Average fluorescence intensity of cell surface VSV-G protein was used to calculate the extent of VSV-G transport.

Data Analysis

Graphs were generated using *Prism Graphpad* version 5. Statistical analysis was performed using *SPSS* version 18. Data with a normal distribution were analyzed using a student t-Test (e.g. colocalization data). Data with a non-normal distribution (e.g. Golgi area/cell area) were analyzed using a Mann-Whitney U test with Bonferroni correction. Data are presented as box and whiskers plots with the box indicating the 25th and 75th percentiles, solid line indicating the median, and the whiskers indicating the 95% confidence intervals.

Supplementary Material

Refer to Web version on PubMed Central for supplementary material.

Acknowledgments

Thanks to Paul Miller, Irina Kaverina, and members of the Weaver laboratory for advice. Funding was provided by NIH grants 1R01GM075126, 1R21DE018244 and ACS grant RSG-118085 to A.M.W., the Vanderbilt International Scholars Award Program (N-H.H.), training grants 5T32 CA009592-23 (K.C.K.) and 1F31DE021619 (L.C.L.). EM image acquisition and analysis at Vanderbilt utilized the VUMC Cell Imaging Shared Resource (supported by NIH grants CA68485, DK20593, DK58404, HD15052, DK59637 and EY08126) and was supported in part by UL1 RR024975 from NCRR/NIH.

References

- Ayala I, Babia T, Baldassarre M, Pompeo A, Fabra A, Kok JW, Luini A, Buccione R, Egea G. Morphological and biochemical analysis of the secretory pathway in melanoma cells with distinct metastatic potential. *FEBS Lett.* 1999; 451(3):315–320. [PubMed: 10371212]
- Bard F, Mazelin L, Pechoux-Longin C, Malhotra V, Jurdic P. Src regulates Golgi structure and KDEL receptor-dependent retrograde transport to the endoplasmic reticulum. *J Biol Chem.* 2003; 278(47): 46601–46606. [PubMed: 12975382]
- Blok J, Mulder-Stapel AA, Daems WT, Ginsel LA. The effect of chloroquine on the intralysosomal degradation of cell-coat glycoproteins in the absorptive cells of cultured human small-intestinal tissue as shown by silver proteinate staining. *Histochemistry.* 1981a; 73(3):429–438. [PubMed: 6173356]
- Blok J, Mulder-Stapel AA, Ginsel LA, Daems WT. The effect of chloroquine on lysosomal function and cell-coat glycoprotein transport in the absorptive cells of cultured human small-intestinal tissue. *Cell Tissue Res.* 1981b; 218(2):227–251. [PubMed: 7261028]

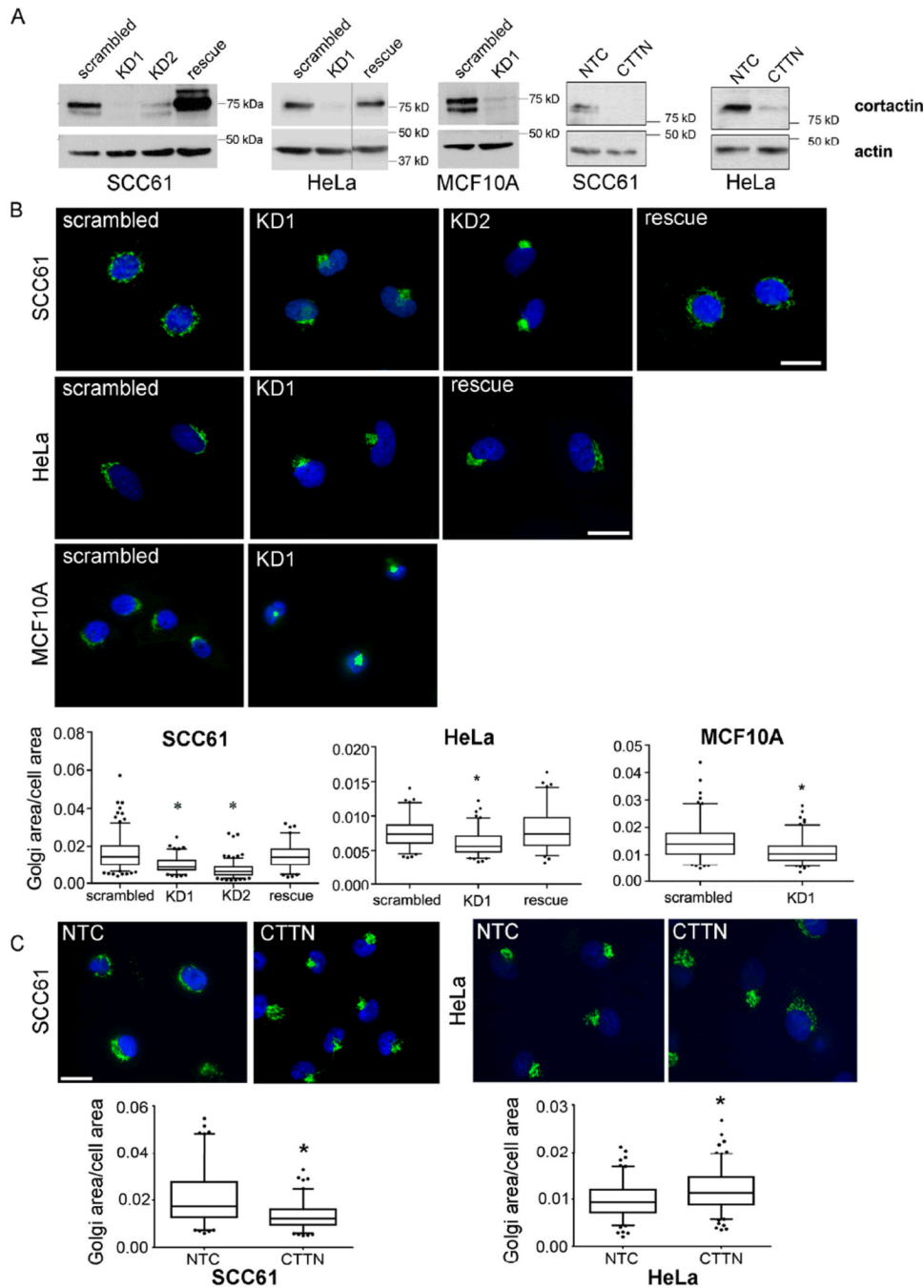
- Brown WJ, Constantinescu E, Farquhar MG. Redistribution of mannose-6-phosphate receptors induced by tunicamycin and chloroquine. *J Cell Biol.* 1984; 99(1 Pt 1):320–326. [PubMed: 6330128]
- Bryce NS, Clark ES, Leysath JL, Currie JD, Webb DJ, Weaver AM. Cortactin promotes cell motility by enhancing lamellipodial persistence. *Curr Biol.* 2005; 15(14):1276–1285. [PubMed: 16051170]
- Burman JL, Hamlin JN, McPherson PS. Scyl1 regulates Golgi morphology. *PLoS One.* 2010; 5(3):e9537. [PubMed: 20209057]
- Campellone KG, Webb NJ, Znameroski EA, Welch MD. WHAMM is an Arp2/3 complex activator that binds microtubules and functions in ER to Golgi transport. *Cell.* 2008; 134(1):148–161. [PubMed: 18614018]
- Cao H, Chen J, Krueger EW, McNiven MA. SRC-mediated phosphorylation of dynamin and cortactin regulates the "constitutive" endocytosis of transferrin. *Mol Cell Biol.* 2010; 30(3):781–792. [PubMed: 19995918]
- Cao H, Orth JD, Chen J, Weller SG, Heuser JE, McNiven MA. Cortactin is a component of clathrin-coated pits and participates in receptor-mediated endocytosis. *Mol Cell Biol.* 2003; 23(6):2162–2170. [PubMed: 12612086]
- Cao H, Weller S, Orth JD, Chen J, Huang B, Chen JL, Stammes M, McNiven MA. Actin and Arf1-dependent recruitment of a cortactin-dynamin complex to the Golgi regulates post-Golgi transport. *Nat Cell Biol.* 2005; 7(5):483–492. [PubMed: 15821732]
- Choudhury A, Dominguez M, Puri V, Sharma DK, Narita K, Wheatley CL, Marks DL, Pagano RE. Rab proteins mediate Golgi transport of caveola-internalized glycosphingolipids and correct lipid trafficking in Niemann-Pick C cells. *J Clin Invest.* 2002; 109(12):1541–1550. [PubMed: 12070301]
- Clark ES, Brown B, Whigham AS, Kochaishvili A, Yarbrough WG, Weaver AM. Aggressiveness of HNSCC tumors depends on expression levels of cortactin, a gene in the 11q13 amplicon. *Oncogene.* 2009; 28(3):431–444. [PubMed: 18931703]
- Clark ES, Weaver AM. A new role for cortactin in invadopodia: Regulation of protease secretion. *Eur J Cell Biol.* 2008
- Clark ES, Whigham AS, Yarbrough WG, Weaver AM. Cortactin is an essential regulator of matrix metalloproteinase secretion and extracellular matrix degradation in invadopodia. *Cancer Res.* 2007; 67(9):4227–4235. [PubMed: 17483334]
- Connolly CN, Futter CE, Gibson A, Hopkins CR, Cutler DF. Transport into and out of the Golgi complex studied by transfecting cells with cDNAs encoding horseradish peroxidase. *J Cell Biol.* 1994; 127(3):641–652. [PubMed: 7962049]
- Derby MC, Lieu ZZ, Brown D, Stow JL, Goud B, Gleeson PA. The trans-Golgi network golgin, GCC185, is required for endosome-to-Golgi transport and maintenance of Golgi structure. *Traffic.* 2007; 8(6):758–773. [PubMed: 17488291]
- di Campli A, Valderrama F, Babia T, De Matteis MA, Luini A, Egea G. Morphological changes in the Golgi complex correlate with actin cytoskeleton rearrangements. *Cell Motil Cytoskeleton.* 1999; 43(4):334–348. [PubMed: 10423274]
- Dippold HC, Ng MM, Farber-Katz SE, Lee SK, Kerr ML, Peterman MC, Sim R, Wiharto PA, Galbraith KA, Madhavarapu S, et al. GOLPH3 bridges phosphatidylinositol-4-phosphate and actomyosin to stretch and shape the Golgi to promote budding. *Cell.* 2009; 139(2):337–351. [PubMed: 19837035]
- Duleh SN, Welch MD. WASH and the Arp2/3 complex regulate endosome shape and trafficking. *Cytoskeleton (Hoboken).* 2010; 67(3):193–206. [PubMed: 20175130]
- Egea G, Lazaro-Dieguex F, Vilella M. Actin dynamics at the Golgi complex in mammalian cells. *Curr Opin Cell Biol.* 2006; 18(2):168–178. [PubMed: 16488588]
- Egorov MV, Capestrano M, Vorontsova OA, Di Pentima A, Egorova AV, Mariggio S, Ayala MI, Tete S, Gorski JL, Luini A, et al. Faciogenital dysplasia protein (FGD1) regulates export of cargo proteins from the golgi complex via Cdc42 activation. *Mol Biol Cell.* 2009; 20(9):2413–2427. [PubMed: 19261807]

- Engqvist-Goldstein AE, Zhang CX, Carreño S, Barroso C, Heuser JE, Drubin DG. RNAi-mediated Hip1R silencing results in stable association between the endocytic machinery and the actin assembly machinery. *Mol Biol Cell*. 2004; 15(4):1666–1679. [PubMed: 14742709]
- Feinstein TN, Linstedt AD. GRASP55 regulates Golgi ribbon formation. *Mol Biol Cell*. 2008; 19(7): 2696–2707. [PubMed: 18434598]
- Fraldi A, Annunziata F, Lombardi A, Kaiser HJ, Medina DL, Spamanato C, Fedele AO, Polishchuk R, Sorrentino NC, Simons K, et al. Lysosomal fusion and SNARE function are impaired by cholesterol accumulation in lysosomal storage disorders. *EMBO J*. 2010; 29(21):3607–3620. [PubMed: 20871593]
- Fucini RV, Chen JL, Sharma C, Kessels MM, Stammes M. Golgi vesicle proteins are linked to the assembly of an actin complex defined by mAbp1. *Mol Biol Cell*. 2002; 13(2):621–631. [PubMed: 11854417]
- Ganley IG, Pfeffer SR. Cholesterol accumulation sequesters Rab9 and disrupts late endosome function in NPC1-deficient cells. *J Biol Chem*. 2006; 281(26):17890–17899. [PubMed: 16644737]
- Grassart A, Meas-Yedid V, Dufour A, Olivo-Marin JC, Dautry-Varsat A, Sauvionnet N. Pak1 phosphorylation enhances Cortactin-N-WASP interaction in clathrin-caveolin-independent endocytosis. *Traffic*. 2010; 11(8):1079–1091. [PubMed: 20444238]
- Guo Y, Linstedt AD. COPII-Golgi protein interactions regulate COPII coat assembly and Golgi size. *J Cell Biol*. 2006; 174(1):53–63. [PubMed: 16818719]
- Hayes GL, Pfeffer SR. WHAMMing into the Golgi. *Dev Cell*. 2008; 15(2):171–172. [PubMed: 18694552]
- Heard JM, Bruyere J, Roy E, Bigou S, Ausseil J, Vitry S. Storage problems in lysosomal diseases. *Biochem Soc Trans*. 2010; 38(6):1442–1447. [PubMed: 21118104]
- Hehnly H, Xu W, Chen JL, Stammes M. Cdc42 regulates microtubule-dependent Golgi positioning. *Traffic*. 2010; 11(8):1067–1078. [PubMed: 20525016]
- Hirschberg K, Miller CM, Ellenberg J, Presley JF, Siggia ED, Phair RD, Lippincott-Schwartz J. Kinetic analysis of secretory protein traffic and characterization of golgi to plasma membrane transport intermediates in living cells. *J Cell Biol*. 1998; 143(6):1485–1503. [PubMed: 9852146]
- Holttu-Vuori M, Alpy F, Tanhuanpaa K, Jokitalo E, Mutka AL, Ikonen E. MLN64 is involved in actin-mediated dynamics of late endocytic organelles. *Mol Biol Cell*. 2005; 16(8):3873–3886. [PubMed: 15930133]
- Huotari J, Helenius A. Endosome maturation. *EMBO J*. 2011; 30(17):3481–3500. [PubMed: 21878991]
- Jerome WG, Cash C, Webber R, Horton R, Yancey PG. Lysosomal lipid accumulation from oxidized low density lipoprotein is correlated with hypertrophy of the Golgi apparatus and trans-Golgi network. *J Lipid Res*. 1998; 39(7):1362–1371. [PubMed: 9684738]
- Kessels MM, Engqvist-Goldstein AE, Drubin DG, Qualmann B. Mammalian Abp1, a signal-responsive F-actin-binding protein, links the actin cytoskeleton to endocytosis via the GTPase dynamin. *J Cell Biol*. 2001; 153(2):351–366. [PubMed: 11309416]
- Kinley AW, Weed SA, Weaver AM, Karginov AV, Bissonette E, Cooper JA, Parsons JT. Cortactin Interacts with WIP in Regulating Arp2/3 Activation and Membrane Protrusion. *Curr Biol*. 2003; 13(5):384–393. [PubMed: 12620186]
- Kirkbride KC, Sung BH, Sinha S, Weaver AM. Cortactin: A multifunctional regulator of cellular invasiveness. *Cell Adh Migr*. 2011; 5(2)
- Klausner RD, Donaldson JG, Lippincott-Schwartz J. Brefeldin A: insights into the control of membrane traffic and organelle structure. *J Cell Biol*. 1992; 116(5):1071–1080. [PubMed: 1740466]
- Kobayashi T, Beuchat MH, Lindsay M, Frias S, Palmiter RD, Sakuraba H, Parton RG, Gruenberg J. Late endosomal membranes rich in lysobisphosphatidic acid regulate cholesterol transport. *Nat Cell Biol*. 1999; 1(2):113–118. [PubMed: 10559883]
- Kokkonen N, Rivinoja A, Kauppila A, Suokas M, Kellokumpu I, Kellokumpu S. Defective acidification of intracellular organelles results in aberrant secretion of cathepsin D in cancer cells. *J Biol Chem*. 2004; 279(38):39982–39988. [PubMed: 15258139]

- Lanzetti L. Actin in membrane trafficking. *Curr Opin Cell Biol.* 2007; 19(4):453–458. [PubMed: 17616384]
- Lazaro-Dieguez F, Jimenez N, Barth H, Koster AJ, Renau-Piqueras J, Llopis JL, Burger KN, Egea G. Actin filaments are involved in the maintenance of Golgi cisternae morphology and intra-Golgi pH. *Cell Motil Cytoskeleton.* 2006; 63(12):778–791. [PubMed: 16960891]
- Lee JY, Koga H, Kawaguchi Y, Tang W, Wong E, Gao YS, Pandey UB, Kaushik S, Tresse E, Lu J, et al. HDAC6 controls autophagosome maturation essential for ubiquitin-selective quality-control autophagy. *EMBO J.* 2010; 29(5):969–980. [PubMed: 20075865]
- Lowe M. Golgi complex: biogenesis de novo? *Curr Biol.* 2002; 12(5):R166–R167. [PubMed: 11882304]
- Martinez-Quiles N, Ho HY, Kirschner MW, Ramesh N, Geha RS. Erk/Src phosphorylation of cortactin acts as a switch on-switch off mechanism that controls its ability to activate N-WASP. *Mol Cell Biol.* 2004; 24(12):5269–5280. [PubMed: 15169891]
- Matas OB, Martinez-Menarguez JA, Egea G. Association of Cdc42/N-WASP/Arp2/3 signaling pathway with Golgi membranes. *Traffic.* 2004; 5(11):838–846. [PubMed: 15479449]
- Merrifield CJ, Perrais D, Zenisek D. Coupling between clathrin-coated-pit invagination, cortactin recruitment, and membrane scission observed in live cells. *Cell.* 2005; 121(4):593–606. [PubMed: 15907472]
- Mukherjee S, Maxfield FR. Lipid and cholesterol trafficking in NPC. *Biochim Biophys Acta.* 2004; 1685(1–3):28–37. [PubMed: 15465424]
- Nakayama Y, Hisano T, Okimoto T, Tanaka Y, Ishikawa T, Himeno M, Ono M, Kuwano M. Microtubule reorganization and lysosome redistribution by a viral v-src oncogene, in mouse Balb/3T3 cells expressing human EGF receptor. *Cell Struct Funct.* 1994; 19(6):397–409. [PubMed: 7720100]
- Narita M, Young AR, Arakawa S, Samarajiwa SA, Nakashima T, Yoshida S, Hong S, Berry LS, Reichelt S, Ferreira M, et al. Spatial coupling of mTOR and autophagy augments secretory phenotypes. *Science.* 2011; 332(6032):966–970. [PubMed: 21512002]
- Novikoff AB, Essner E, Quintana N. Golgi Apparatus and Lysosomes. *Fed Proc.* 1964; 23:1010–1022.
- Ohashi E, Tanabe K, Henmi Y, Mesaki K, Kobayashi Y, Takei K. Receptor sorting within endosomal trafficking pathway is facilitated by dynamic actin filaments. *PLoS One.* 2011; 6(5):e19942. [PubMed: 21625493]
- Onabajo OO, Seeley MK, Kale A, Qualmann B, Kessels M, Han J, Tan TH, Song W. Actin-binding protein 1 regulates B cell receptor-mediated antigen processing and presentation in response to B cell receptor activation. *J Immunol.* 2008; 180(10):6685–6695. [PubMed: 18453588]
- Pfeffer SR. Multiple routes of protein transport from endosomes to the trans Golgi network. *FEBS Lett.* 2009; 583(23):3811–3816. [PubMed: 19879268]
- Ponnambalam S, Baldwin SA. Constitutive protein secretion from the trans-Golgi network to the plasma membrane. *Mol Membr Biol.* 2003; 20(2):129–139. [PubMed: 12851070]
- Presley JF, Cole NB, Schroer TA, Hirschberg K, Zaal KJ, Lippincott-Schwartz J. ER-to-Golgi transport visualized in living cells. *Nature.* 1997; 389(6646):81–85. [PubMed: 9288971]
- Press B, Feng Y, Hoflack B, Wandinger-Ness A. Mutant Rab7 causes the accumulation of cathepsin D and cation-independent mannose 6-phosphate receptor in an early endocytic compartment. *J Cell Biol.* 1998; 140(5):1075–1089. [PubMed: 9490721]
- Pulvirenti T, Giannotta M, Capestrano M, Capitani M, Pisanu A, Polishchuk RS, San Pietro E, Beznoussenko GV, Mironov AA, Turacchio G, et al. A traffic-activated Golgi-based signalling circuit coordinates the secretory pathway. *Nat Cell Biol.* 2008; 10(8):912–922. [PubMed: 18641641]
- Putthenveedu MA, Lauffer B, Temkin P, Vistein R, Carlton P, Thorn K, Taunton J, Weiner OD, Parton RG, von Zastrow M. Sequence-dependent sorting of recycling proteins by actin-stabilized endosomal microdomains. *Cell.* 2010; 143(5):761–773. [PubMed: 21111236]
- Quinn P, Griffiths G, Warren G. Dissection of the Golgi complex. II. Density separation of specific Golgi functions in virally infected cells treated with monensin. *J Cell Biol.* 1983; 96(3):851–856. [PubMed: 6403555]

- Reddy JV, Burguete AS, Sridevi K, Ganley IG, Nottingham RM, Pfeffer SR. A functional role for the GCC185 golgin in mannose 6-phosphate receptor recycling. *Mol Biol Cell*. 2006; 17(10):4353–4363. [PubMed: 16885419]
- Salvarezza SB, Deborde S, Schreiner R, Campagne F, Kessels MM, Qualmann B, Caceres A, Kreitzer G, Rodriguez-Boulan E. LIM kinase 1 and cofilin regulate actin filament population required for dynamin-dependent apical carrier fission from the trans-Golgi network. *Mol Biol Cell*. 2009; 20(1):438–451. [PubMed: 18987335]
- Sandilands E, Frame MC. Endosomal trafficking of Src tyrosine kinase. *Trends Cell Biol*. 2008; 18(7): 322–329. [PubMed: 18515107]
- Sauvonnet N, Dujeancourt A, Dautry-Varsat A. Cortactin and dynamin are required for the clathrinin-dependent endocytosis of $\{\gamma\}$ cytokine receptor. *J Cell Biol*. 2005; 168(1):155–163. [PubMed: 15623579]
- Sbai O, Ould-Yahoui A, Ferhat L, Gueye Y, Bernard A, Charrat E, Mehanna A, Risso JJ, Chauvin JP, Fenouillet E, et al. Differential vesicular distribution and trafficking of MMP-2, MMP-9, and their inhibitors in astrocytes. *Glia*. 2009; 58(3):344–366. [PubMed: 19780201]
- Steffen A, Le Dez G, Poincloux R, Recchi C, Nassoy P, Rottner K, Galli T, Chavrier P. MT1-MMP-dependent invasion is regulated by TI-VAMP/VAMP7. *Curr Biol*. 2008; 18(12):926–931. [PubMed: 18571410]
- Sung BH, Zhu X, Kaverina I, Weaver AM. Cortactin Controls Cell Motility and Lamellipodial Dynamics by Regulating ECM Secretion. *Curr Biol*. 2011
- Valderrama F, Babia T, Ayala I, Kok JW, Renau-Piqueras J, Egea G. Actin microfilaments are essential for the cytological positioning and morphology of the Golgi complex. *Eur J Cell Biol*. 1998; 76(1):9–17. [PubMed: 9650778]
- Valderrama F, Duran JM, Babia T, Barth H, Renau-Piqueras J, Egea G. Actin microfilaments facilitate the retrograde transport from the Golgi complex to the endoplasmic reticulum in mammalian cells. *Traffic*. 2001; 2(10):717–726. [PubMed: 11576448]
- Valderrama F, Luna A, Babia T, Martinez-Menarguez JA, Ballesta J, Barth H, Chaponnier C, Renau-Piqueras J, Egea G. The golgi-associated COPI-coated buds and vesicles contain beta/gamma - actin. *Proc Natl Acad Sci U S A*. 2000; 97(4):1560–1565. [PubMed: 10677499]
- Vanlandingham PA, Ceresa BP. Rab7 regulates late endocytic trafficking downstream of multivesicular body biogenesis and cargo sequestration. *J Biol Chem*. 2009; 284(18):12110–12124. [PubMed: 19265192]
- Vincent C, Maridonneau-Parini I, Le Clainche C, Gounon P, Labrousse A. Activation of p61Hck triggers WASp- and Arp2/3-dependent actin-comet tail biogenesis and accelerates lysosomes. *J Biol Chem*. 2007; 282(27):19565–19574. [PubMed: 17500055]
- Vitry S, Bruyere J, Hocquemiller M, Bigou S, Ausseil J, Colle MA, Prevost MC, Heard JM. Storage vesicles in neurons are related to Golgi complex alterations in mucopolysaccharidosis IIIB. *Am J Pathol*. 2010; 177(6):2984–2999. [PubMed: 21037080]
- von Blume J, Duran JM, Forlanelli E, Alleaume AM, Egorov M, Polishchuk R, Molina H, Malhotra V. Actin remodeling by ADF/cofilin is required for cargo sorting at the trans-Golgi network. *J Cell Biol*. 2009; 187(7):1055–1069. [PubMed: 20026655]
- Warner CL, Stewart A, Luzio JP, Steel KP, Libby RT, Kendrick-Jones J, Buss F. Loss of myosin VI reduces secretion and the size of the Golgi in fibroblasts from Snell's waltzer mice. *EMBO J*. 2003; 22(3):569–579. [PubMed: 12554657]
- Weaver AM. Invadopodia: specialized cell structures for cancer invasion. *Clin Exp Metastasis*. 2006; 23(2):97–105. [PubMed: 16830222]
- Weed SA, Karginov AV, Schafer DA, Weaver AM, Kinley AW, Cooper JA, Parsons JT. Cortactin localization to sites of actin assembly in lamellipodia requires interactions with F-actin and the Arp2/3 complex. *J Cell Biol*. 2000; 151(1):29–40. [PubMed: 11018051]
- Weed SA, Parsons JT. Cortactin: coupling membrane dynamics to cortical actin assembly. *Oncogene*. 2001; 20(44):6418–6434. [PubMed: 11607842]
- Weibel, ER. *Stereological Methods*. New York: Academic Press; 1979. I. Practical Methods for Biological Morphometry.

- Weibel ER, Staubli W, Gnagi HR, Hess FA. Correlated morphometric and biochemical studies on the liver cell. I. Morphometric model, stereologic methods, and normal morphometric data for rat liver. *J Cell Biol.* 1969; 42(1):68–91. [PubMed: 4891915]
- Weller SG, Capitani M, Cao H, Micaroni M, Luini A, Sallese M, McNiven MA. Src kinase regulates the integrity and function of the Golgi apparatus via activation of dynamin 2. *Proc Natl Acad Sci U S A.* 2010; 107(13):5863–5868. [PubMed: 20231454]
- Wu H, Reynolds AB, Kanner SB, Vines RR, Parsons JT. Identification and characterization of a novel cytoskeleton-associated pp60src substrate. *Mol Cell Biol.* 1991; 11(10):5113–5124. [PubMed: 1922035]
- Xu W, Stammes M. The actin-depolymerizing factor homology and charged/helical domains of drebrin and mAbp1 direct membrane binding and localization via distinct interactions with actin. *J Biol Chem.* 2006; 281(17):11826–11833. [PubMed: 16452483]
- Zhang M, Chen L, Wang S, Wang T. Rab7: roles in membrane trafficking and disease. *Biosci Rep.* 2009; 29(3):193–209. [PubMed: 19392663]
- Zhu J, Yu D, Zeng XC, Zhou K, Zhan X. Receptor-mediated endocytosis involves tyrosine phosphorylation of cortactin. *J Biol Chem.* 2007; 282(22):16086–16094. [PubMed: 17420251]
- Zhu J, Zhou K, Hao JJ, Liu J, Smith N, Zhan X. Regulation of cortactin/dynamin interaction by actin polymerization during the fission of clathrin-coated pits. *J Cell Sci.* 2005; 118(Pt 4):807–817. [PubMed: 15671060]

**Figure 1. Cortactin regulates Golgi morphology**

A. Immunoblot of cortactin expression (top panels) and β -actin loading control (bottom panels) in SCC61, HeLa and MCF10A stable (3 left panels) or transient (2 right panels) KD cell lines. For the transient siRNA experiments NTC indicates nontargeting control and CTTN indicates cortactin-specific siRNA. **B.** Representative images and analyses of SCC61 cells (top), HeLa cells (middle) and MCF10A cells (bottom) stably expressing control shRNA (scrambled), human cortactin-specific shRNA (KD1, KD2), or cortactin-KD1 plus shRNA-resistant wild-type mouse cortactin (rescue) and immunostained for the Golgi marker, GM130 (green), actin filaments (rhodamine-phalloidin, not shown) and the nucleus (Hoechst, blue). Graphs show quantification of the ratio of Golgi area to total cell area of

individual cells. **C.** Representative images and analyses of transient control (NTC) or cortactin-KD (CTTN) SCC61 or HeLa cells. Scale bar = 25 μ m. For each condition, n = 20 cells from each of 3 independent experiments. Data are presented as box and whiskers plots with the box indicating the 25th and 75th percentiles, solid line indicating the median, and the whiskers indicating the 95% confidence intervals.*p<0.05.

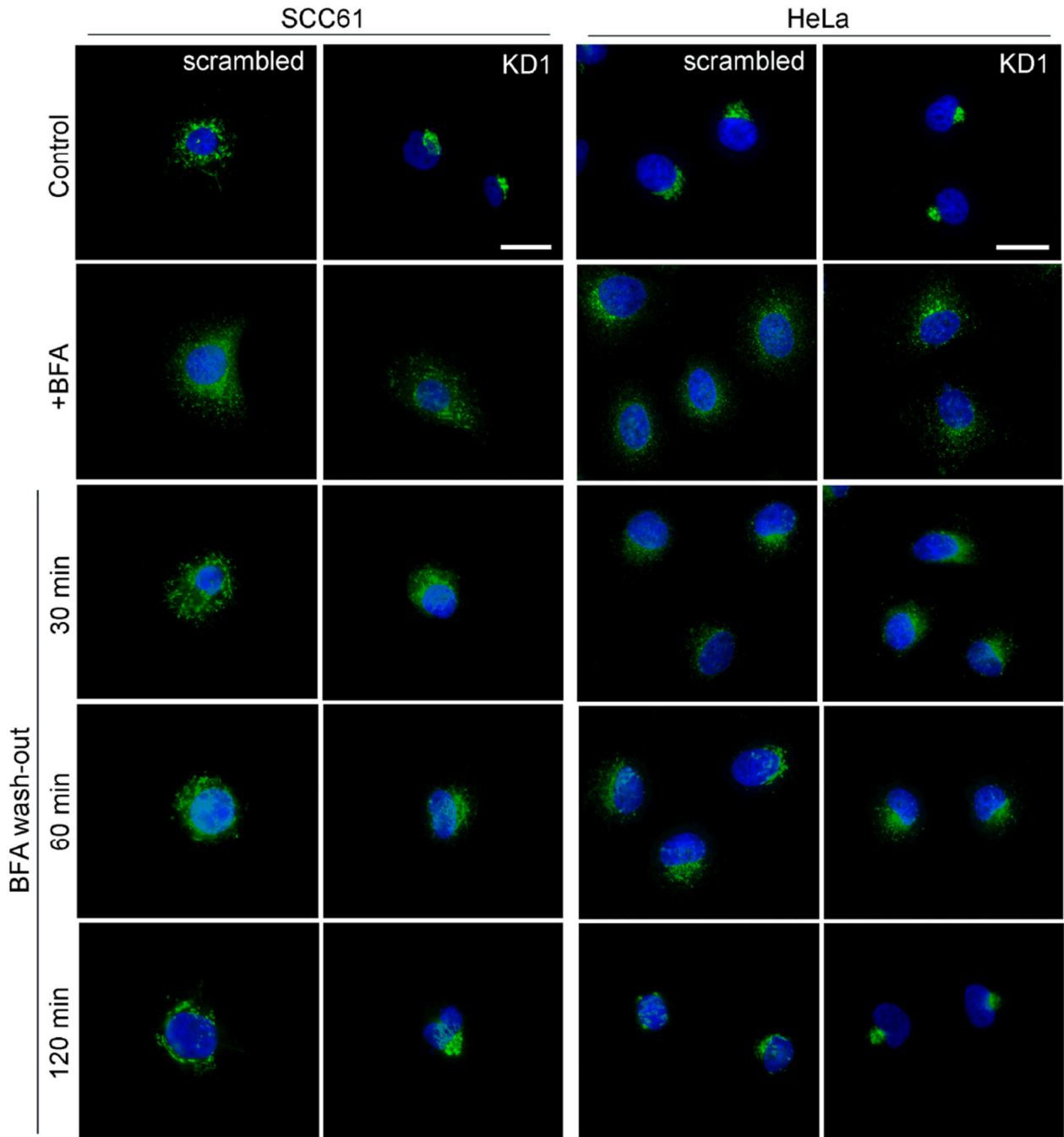


Figure 2. Loss of cortactin does not disrupt Golgi disassembly or reassembly

SCC61 (left panels) and HeLa (right panels) scrambled and KD1 cells were treated with Brefeldin A (5 µg/ml, “+BFA”) for 30 minutes, followed by replacing the media with serum-containing media (“wash-out”) for the indicated times. The cells were fixed and the Golgi and nuclei were stained using GM130 (green) and Hoechst (blue), respectively. Representative images are shown. Compare 120 min timepoint to vehicle-treated cells (“Control”). n = 2 independent experiments. Scale bars = 25 µm.

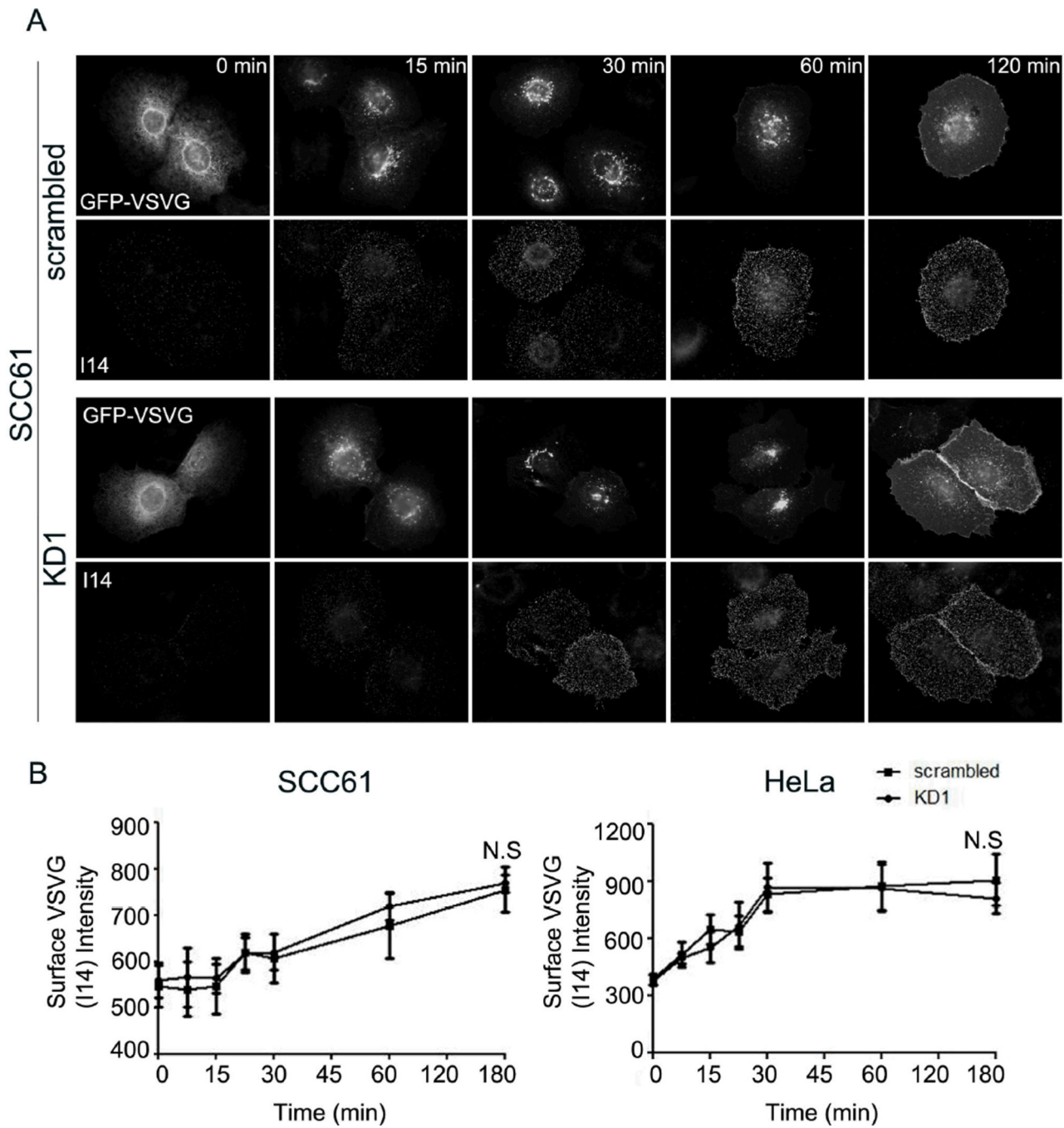


Figure 3. Cortactin-KD does not affect transport of VSV-G to the plasma membrane

Transport of ts045-VSV-G-GFP (VSV-G) to the plasma membrane was assessed over a 3-h period following a shift of the cells to the permissive temperature of 32°C in SCC61 or HeLa cells expressing either control (scrambled) or cortactin-specific shRNA (KD1).

A. Representative images showing total expressed VSV-G (green) and cell surface I14-detected VSV-G (red) in SCC61 cells as a function of time. Images for HeLa cells are shown in Figure S5. **B.** Analysis of the average surface intensity of I14 VSV-G staining at each time point after the shift to 32°C for SCC61 (left) or HeLa (right) cells. n=3; >20 cells per independent experiment at each time point. N.S. = Not significant. Scale bar = 25 μm.

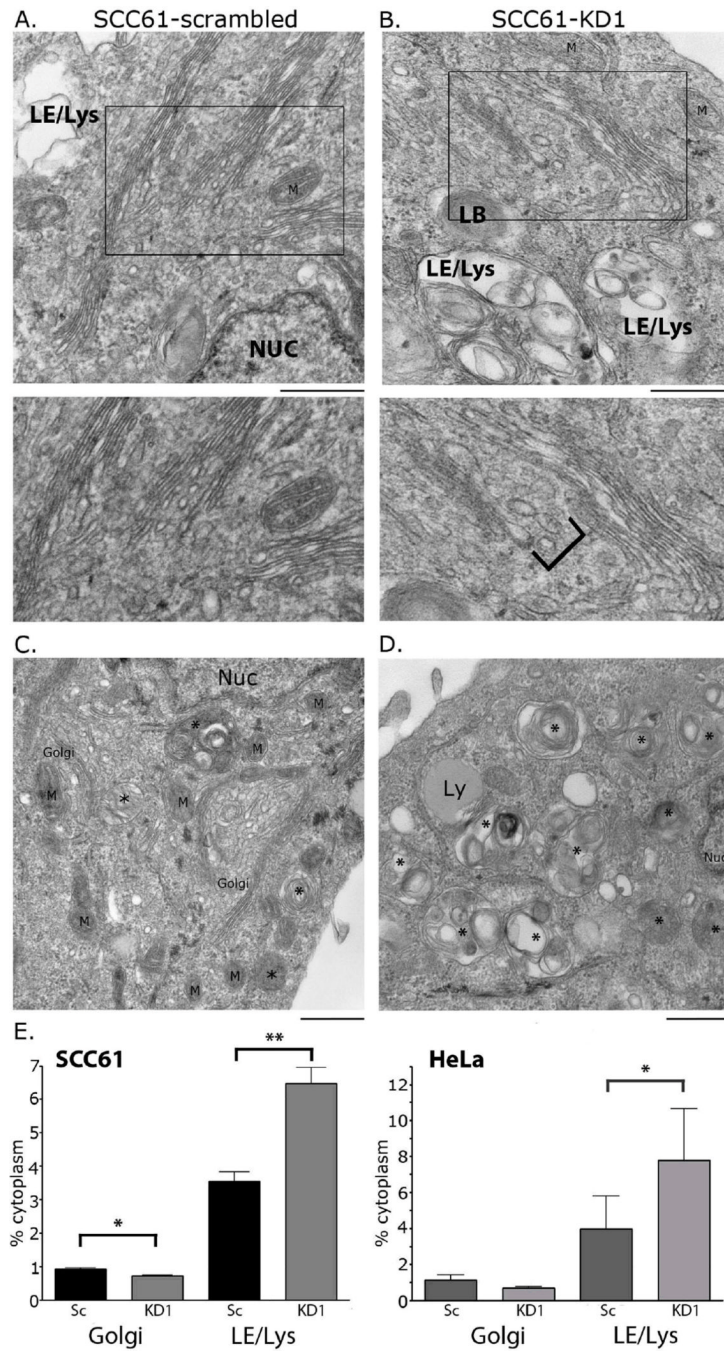


Figure 4. Cortactin-KD cells contain many LE/Lys hybrid organelles and have little perturbation in Golgi structure or volume

Transmission electron microscopy was performed on 50 nm thick cellular sections. **A, B.** Representative images of the overall Golgi morphology in SCC61-scrambled (A) and SCC61 cortactin-KD1 (B) cells. Note the increase in LE/Lys and lamellar bodies (LB) within KD cells. NUC = nucleus. ZOOMS of the Golgi shown below A and B. An increase in trans-Golgi-associated vesicles in KD cells is indicated with a bracket. **C, D.** Representative images of the cytoplasmic contents of control (C) and cortactin-knockdown (D) SCC61 cells. LE/Lys and LB are indicated by * in C and D). Scale bar = 500 nm. **E.** % Cytoplasmic volume occupied by Golgi or LE/Lys was analyzed by point counting stereology of random

thin sections and plotted. N = 3 sections, from 2 independent blocks. For representative HeLa images, see Fig S2B–E. Mean \pm SE shown. * p<0.05, **p<0.01.

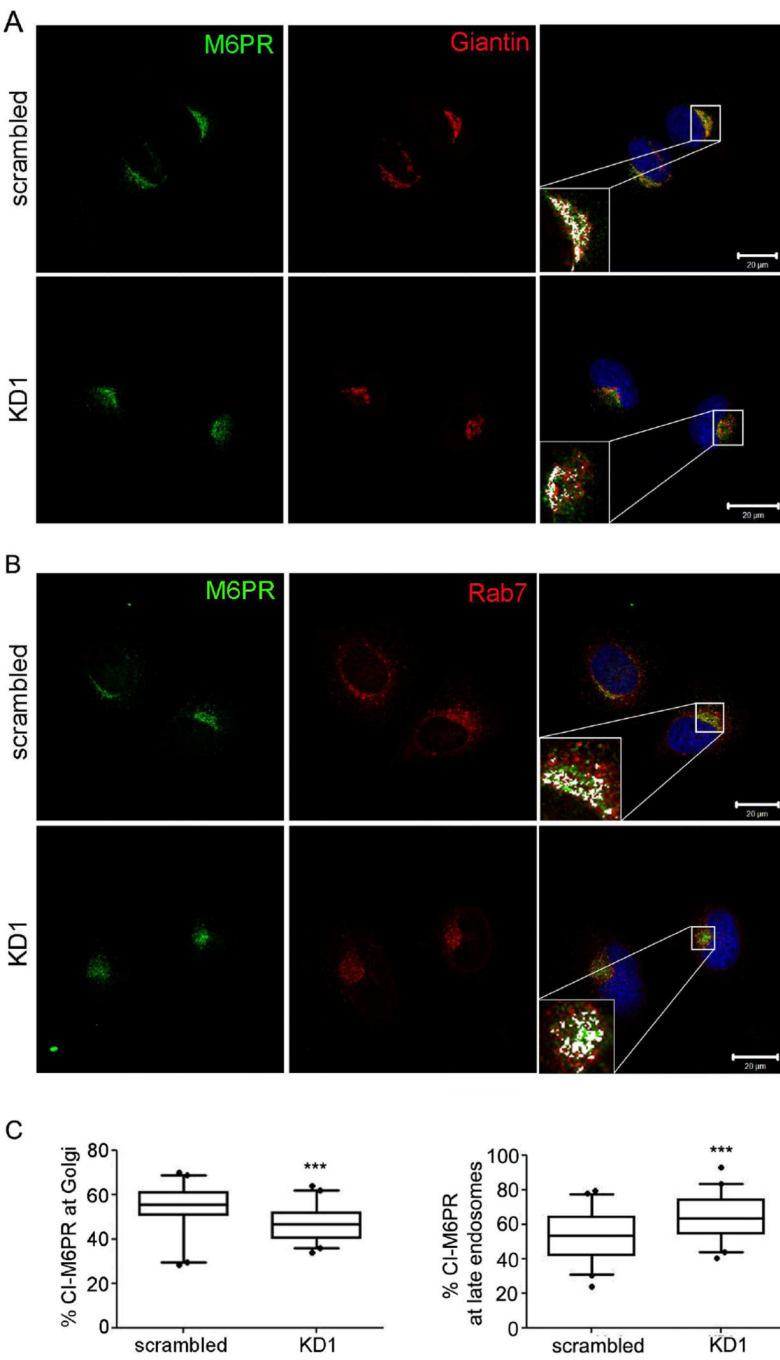


Figure 5. Depletion of cortactin leads to accumulation of Mannose-6-Phosphate Receptor (M6PR) in a late endosomal compartment and depletion from the Golgi
A and B. HeLa cells were stained for M6PR (CI-M6PR) and either Golgi marker Giantin (A) or late endosomal marker Rab7 (B). Boxed areas are zoomed to show colocalization of M6PR with Giantin or Rab7. Colocalized single pixels (white) were visualized using colocalization ImageJ plugin. Scale bars = 20 μ m. C. Images were analyzed for % colocalization of M6PR with Giantin or Rab7. n=3; >15 cells per independent experiments. Data are presented as box and whiskers plots with the box indicating the 25th and 75th percentiles, solid line indicating the median, and the whiskers indicating the 95% confidence intervals. ***p<0.001

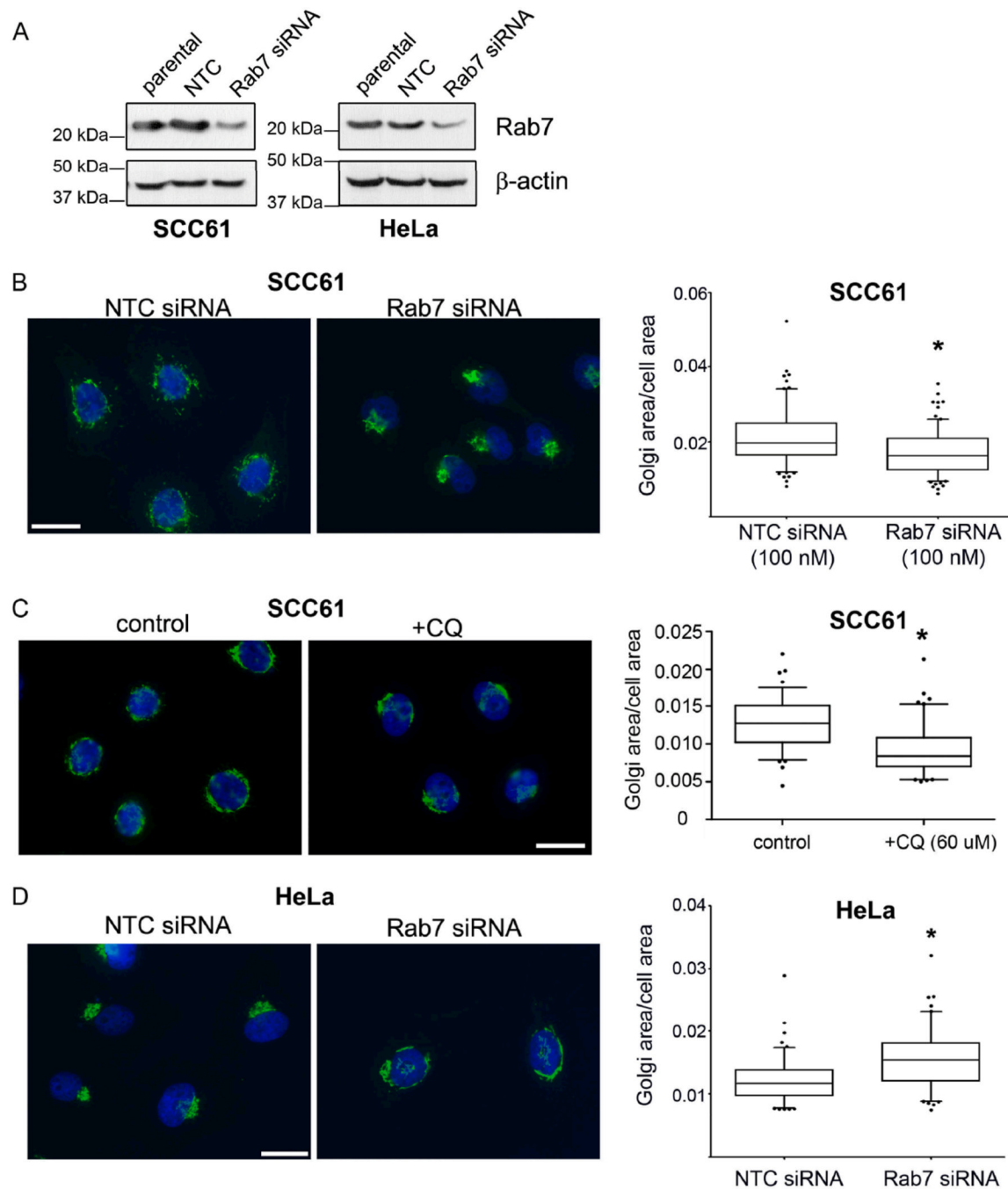


Figure 6. Inhibition of late endosomal/lysosomal trafficking leads to a compact Golgi morphology

A. Representative immunoblot of Rab7 expression levels (top panels) in SCC61 parental cells and those transiently transfected with non-targeting control siRNA (NTC) or Rab7a-specific siRNA, along with a β-actin control. **B.** Rab7-KD reduces Golgi size in SCC61 cells. Representative images (green=GM130, blue=Hoechst) and analysis. **C.** Chloroquine treatment in SCC61 cells reduces Golgi size. Representative images and analysis of SCC61 parental cells treated with either vehicle (water, “control”) or chloroquine (60 μM, “CQ”) for 12 hours. **D.** Rab7-KD causes an increase in Golgi size in HeLa cells. Representative images and corresponding analysis. Scale bar= 25 μm. n=3, with >30 cells per independent experiment

experiment. Data are presented as box and whiskers plots with the box indicating the 25th and 75th percentiles, solid line indicating the median, and the whiskers indicating the 95% confidence intervals.*p<0.05.

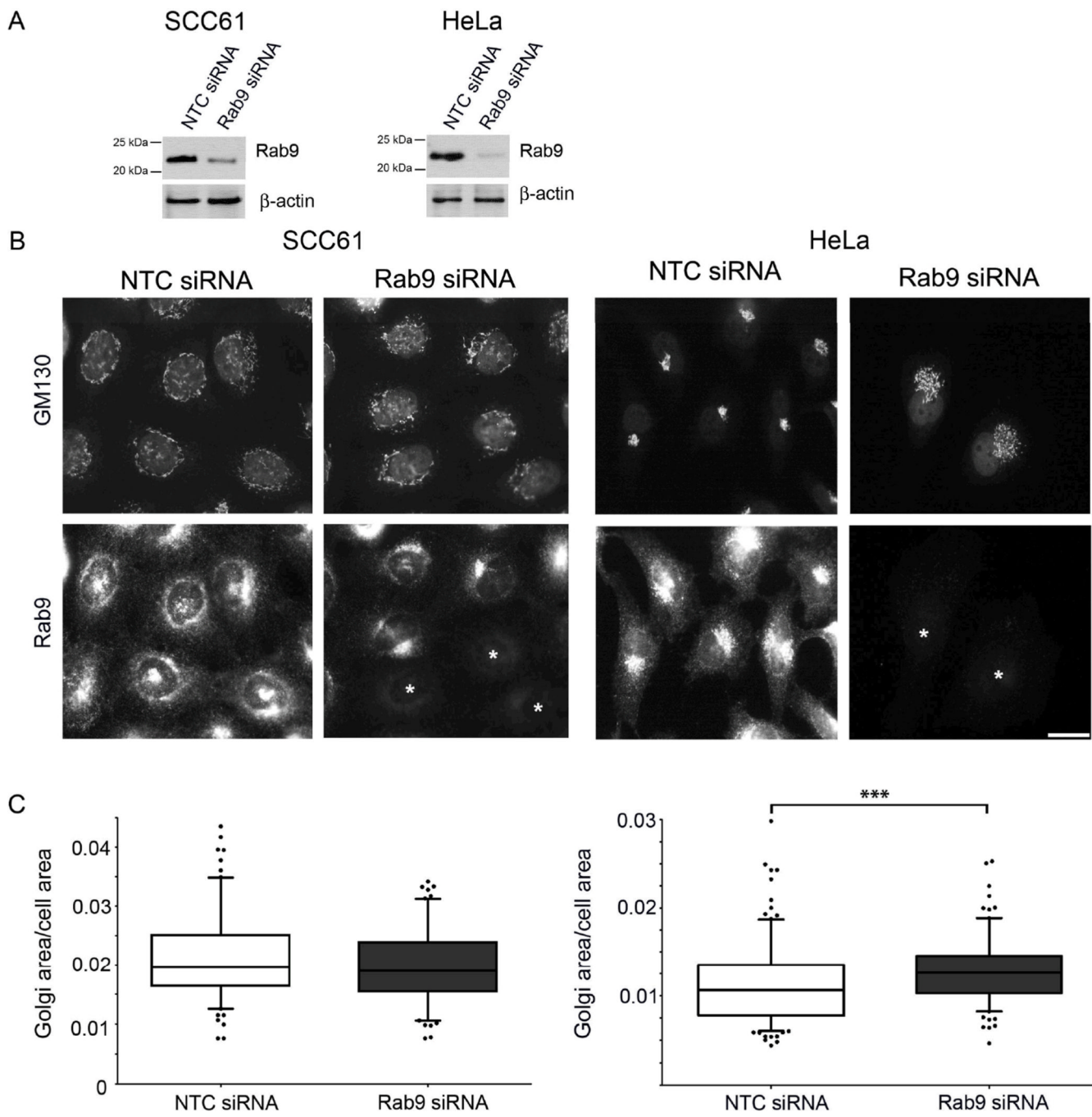


Figure 7. Loss of Rab9 does not phenocopy cortactin-KD

A. Western blot analysis of Rab9 (top) and b-actin (bottom) from total cell lysates of SCC61 (left) or HeLa (right) cells transfected with the Rab9 siRNA. **B.** Representative immunofluorescence images of GM130 staining (top panels) and Rab9 (bottom panels) in transfected cells. Asterisk (*) indicates cells with Rab9 knockdown. **C.** Ratio of Golgi area to total cell area including all the data (>130 cells) from 3 independent experiments (>38 cells per independent experiment). Scale bar = 25 μ m. Data are presented as box and whiskers plots with the box indicating the 25th and 75th percentiles, solid line indicating the median, and the whiskers indicating the 95% confidence intervals. ***p<0.001

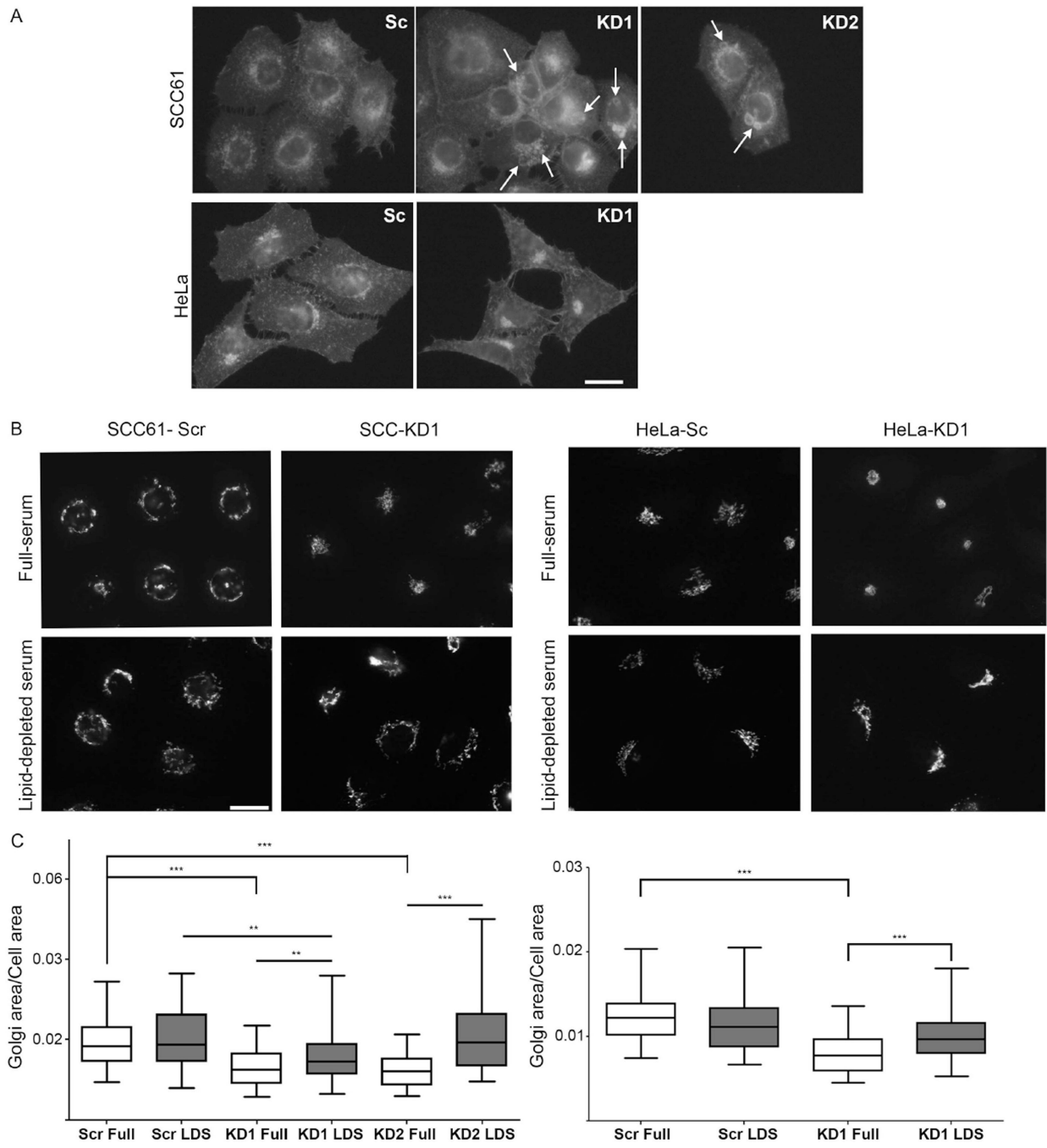


Figure 8. Lipid-depletion rescues Golgi morphology defects in cortactin-KD cells

A. Representative images of SCC61 (top panels) and HeLa (lower panels) control (Scr) and cortactin-KD (KD1, KD2) cells stained for free cholesterol with filipin. Arrows point to large filipin-positive vacuoles and vesicular compartments. **B.** Representative images of GM130 immunofluorescence in cells cultured in full serum (top panels) and lipid-depleted serum (LDS, bottom panels). **C.** Ratio of Golgi area to total cell area for SCC61 cells (left) and HeLa cells (right) in full serum or LDS. $n = 3$, with >22 cells per independent experiment; all data plotted (>85 cells per cell line). Scale bar = $25 \mu\text{m}$. Data are presented as box and whiskers plots with the box indicating the 25th and 75th percentiles, solid line

indicating the median, and the whiskers indicating the 95% confidence intervals. ** $p<0.01$; *** $p<0.001$.

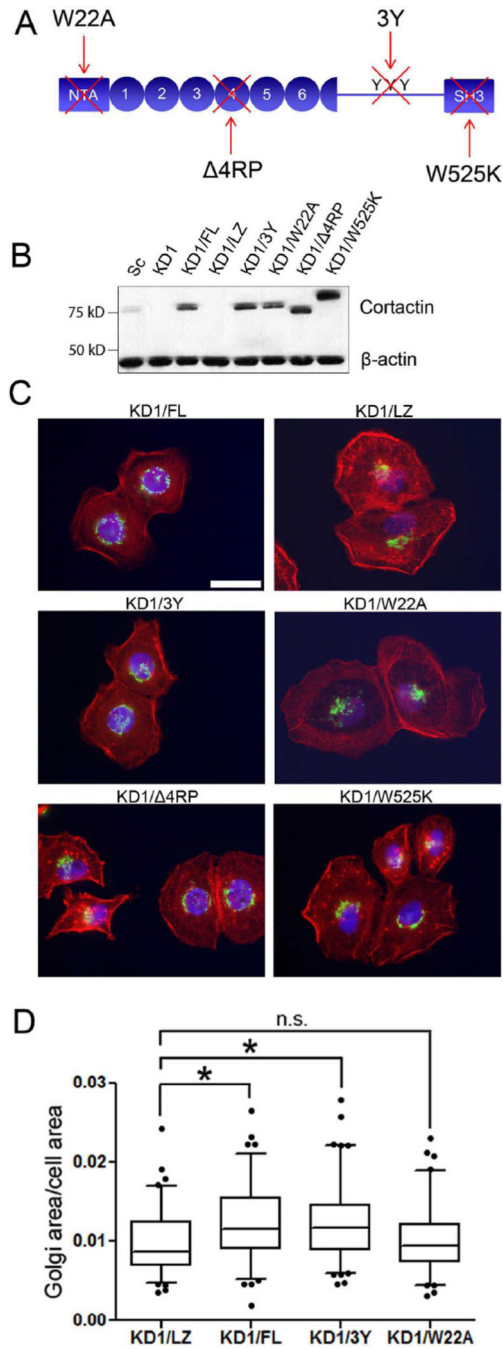


Figure 9. Cortactin binding to the Arp2/3 complex is critical for regulation of Golgi morphology

A. Schematic of cortactin with mutant sites indicated: W22A (Arp2/3 binding mutant); 3Y (Src phosphorylation mutant); Δ4RP (F-actin binding mutant); and W525K (SH3 binding mutant). NTA represents the N-terminal acidic domain, YYY represents Src phosphorylation sites, and circles represent cortactin repeat domains. For B-D: FL = wild-type cortactin, LZ = empty vector, Sc = scrambled oligo. Others as indicated in A. **B.** Western blot analysis of cortactin mutant expression (top panel) and actin as a loading control (bottom panel) in stable SCC61 cells. **C.** Representative widefield images of the Golgi (GM130, green), actin (rhodamine-phalloidin, red) and Hoechst (blue) in the cortactin

mutants. **D.** Quantitation of Golgi area to cell area ratio from n=3; >20 cells per independent experiment. Scale bar = 25 μ m. Data are presented as box and whiskers plots with the box indicating the 25th and 75th percentiles, solid line indicating the median, and the whiskers indicating the 95% confidence intervals. *p<0.05